Infrared Photometry for Automated Telescopes: Passband Selection

Eugene F. Milone (Univ. of Calgary)
Andrew T. Young (SDSU)

Telescopes from AFAR Conference, Waikoloa, Hawaii, Feb. 28-Mar . 3, 2011

Atmospheric Windows

- Ground-based Infrared Photometry
  is constrained by non-transparent spectrum
  atmospheric absorbers (mainly water vapor).

- Rayleigh scattering, important for visual photometry, is much less important.

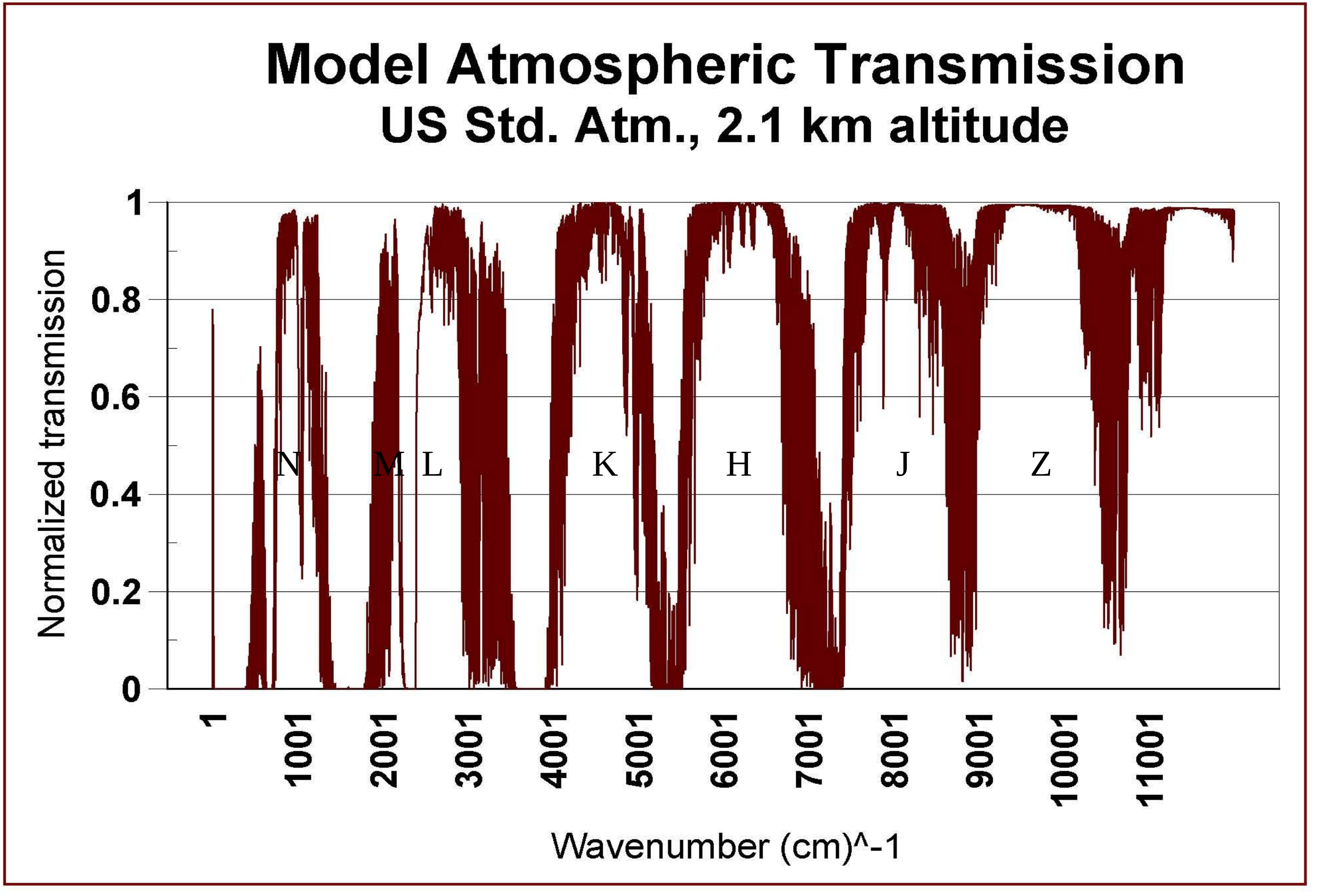

SPECTRAL WINDOWS

The Promise of IR Photometry

Infrared photometry can produce the high photometric precision because:

little Rayleigh scattering ($\propto \lambda^{-4}$), and

compensation for (relatively high) sky brightness

High IR precision has not been achieved, partly because:

photometric astronomers are reluctant to get into IR:

- technical challenges (including cryogenics), and
- filters in common use are not optimized to avoid water-vapor absorptions --- the main impediment to precise ground-based IR photometry.

The original Johnson J passbands demonstrates …

Z, J Windows

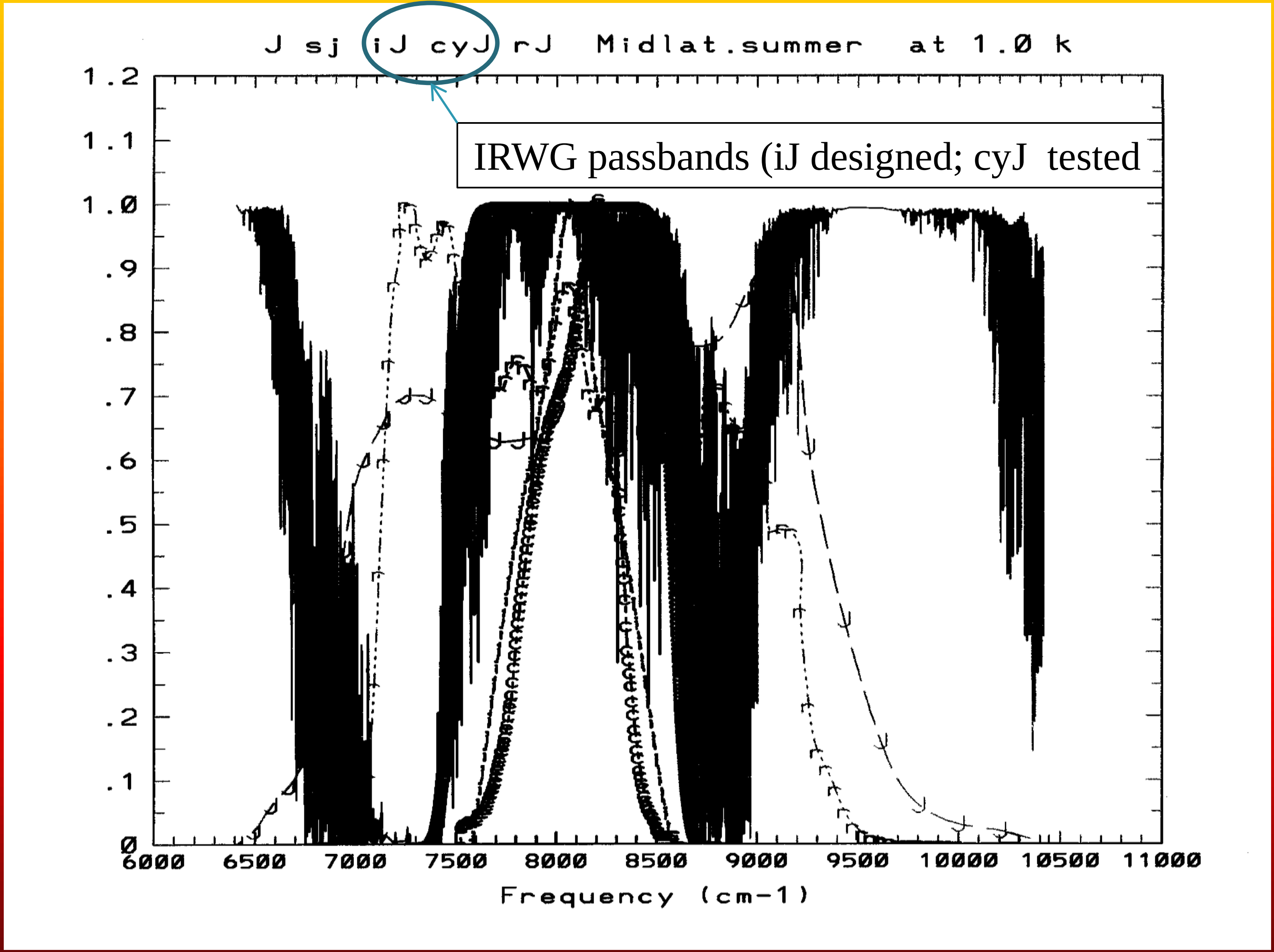

J sj iJ cyJ rJ Midlat.summer at 1.Ø k
IRWG passbands (iJ designed; cyJ tested
1.2
1.1
1.Ø
.9
.8
.7
.6
.5
.4
.3
.2
.1
Ø
6ØØØ
65ØØ
7ØØØ
75ØØ
8ØØØ
85ØØ
9ØØØ
95ØØ
1ØØØØ
1Ø5ØØ
11ØØØ
Frequency (cm-1)

Time Line

- 1987: Milone suggests to Rufener a meeting to discuss IR extinction & standardization
- 1988: Joint Commission meeting at Baltimore GA recommends action; WG formed
- 1991: Mclean commissions formal IRWG
- 1992: Preliminary results reported in IAUC 138
- 1993: Barr Assocs. promises but does not deliver
- 1994: YMS paper in A&A presents new passbands
- 1999: IRWG filters made by Custom Scientific
- 2002: Simons' Gemini filters (MKO-NIR) mass buy!
- 2005: YM paper with list of IRWG standards
- 2012: Mass buy of IRWG filters?
- 2012: Longer WL IRWG filters produced, used?

Simulated J Extinction Curves

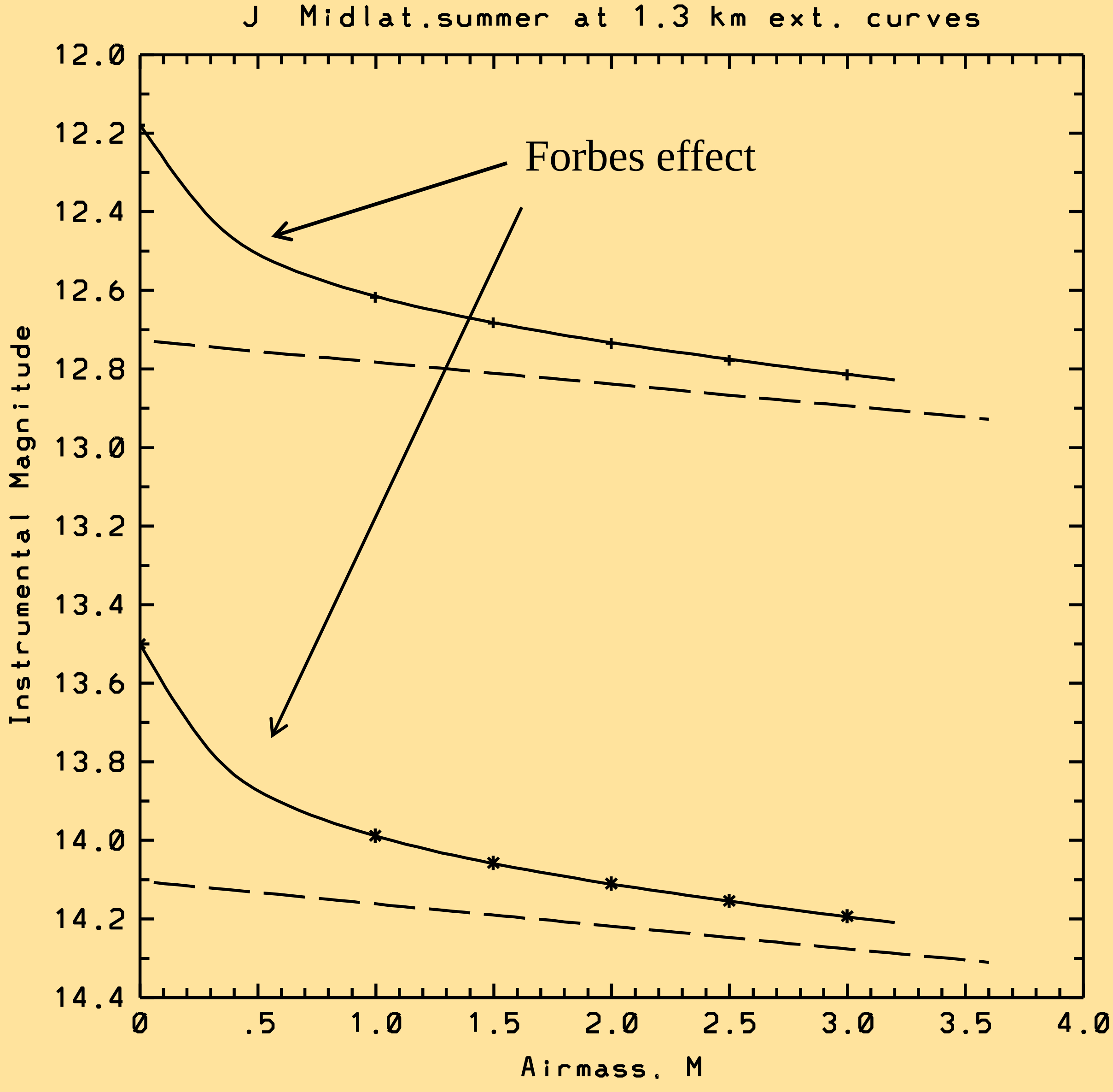

Two source stars with log g = 0:
top: T_{eff} = 3500 K
bottom: 5750 K

Advantages of the IRWG Passbands

The fix: IRWG passbands are **not** defined by the edges of the atmospheric windows

➔they admit no flux from these (constantly varying) edges.

Trade-off costs for improved precision:

- lower throughput
- higher costs for the filters, if made in small lots

Why these should be paid:

1. higher precision
2. improved signal-to-noise ratio
3. lower extinction
4. minimal curvature of extinction curve high in atmosphere

➔ higher precision + accuracy in extra-atmospheric magnitudes.

IRWG iJ passband Extinction Curves

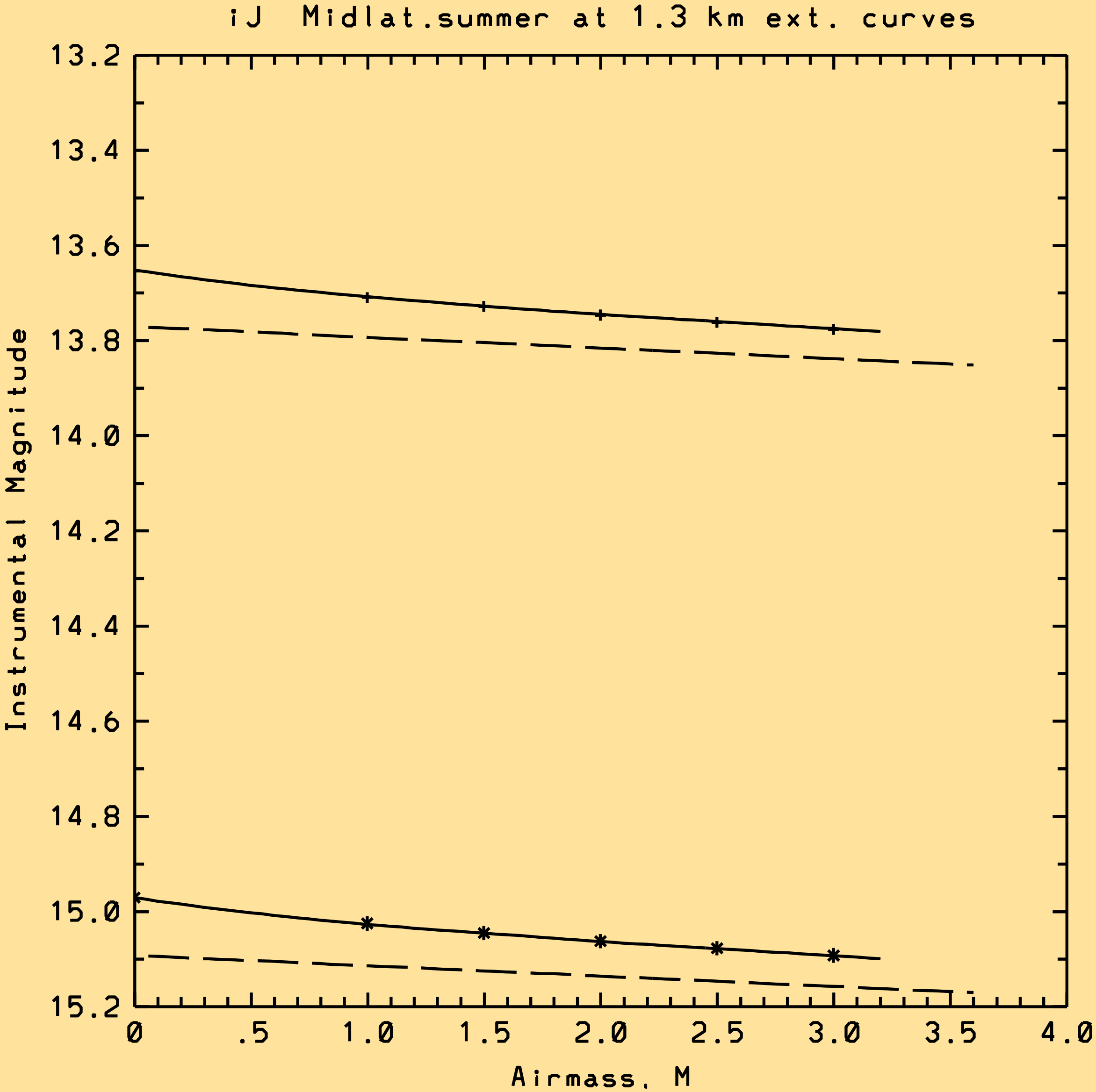

N.B.: same stellar sources as J curves. Note decreased Forbes effect for a passband optimally fitted to the atmospheric window.

z, J Window Passband Quality

Theta vs. Forbes effect, 1 km., mid-summer atm. model

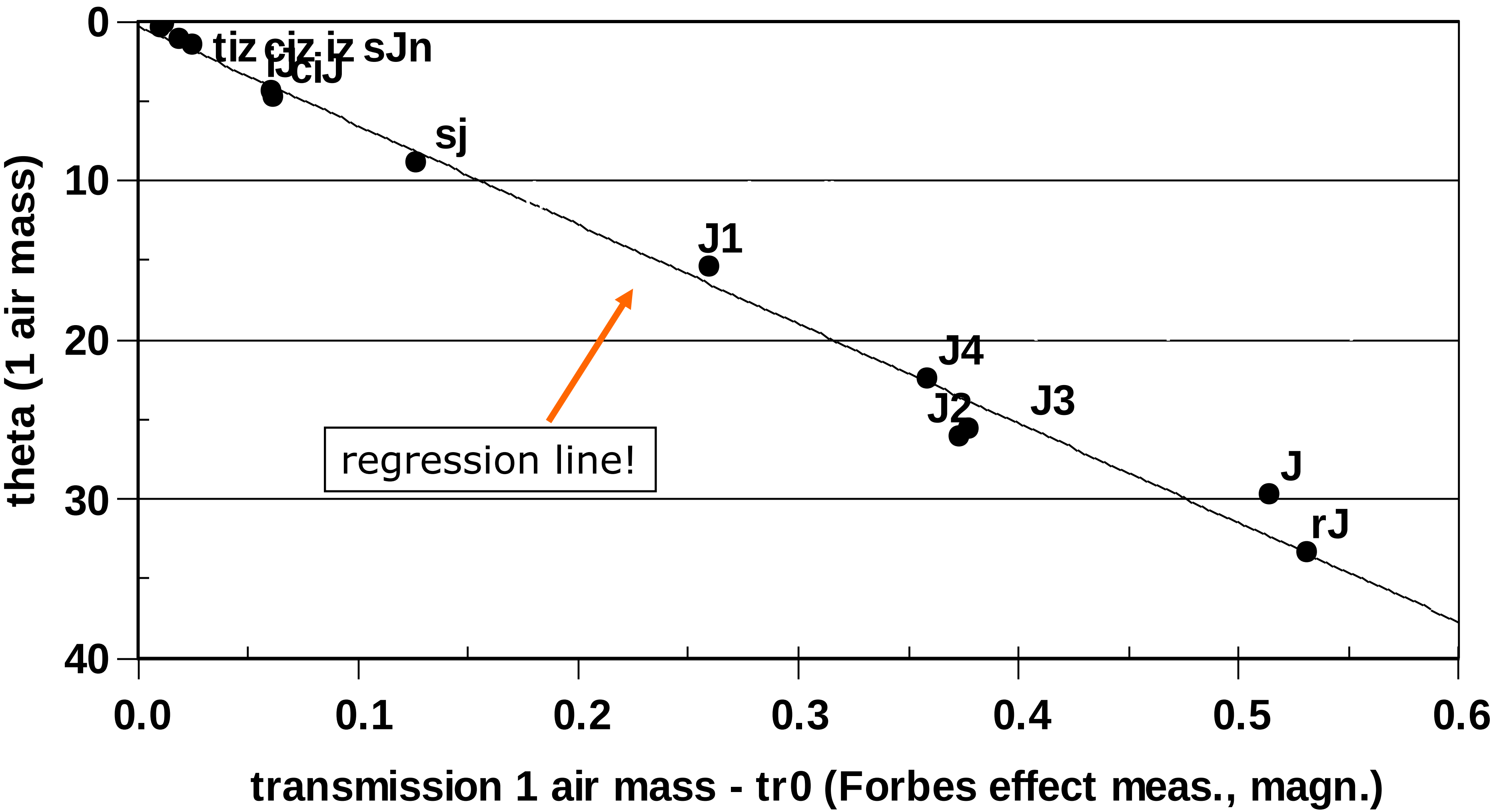

theta: measure of distortion in flux bundle from atm. water vapor

Relationship between SNR & Extinction

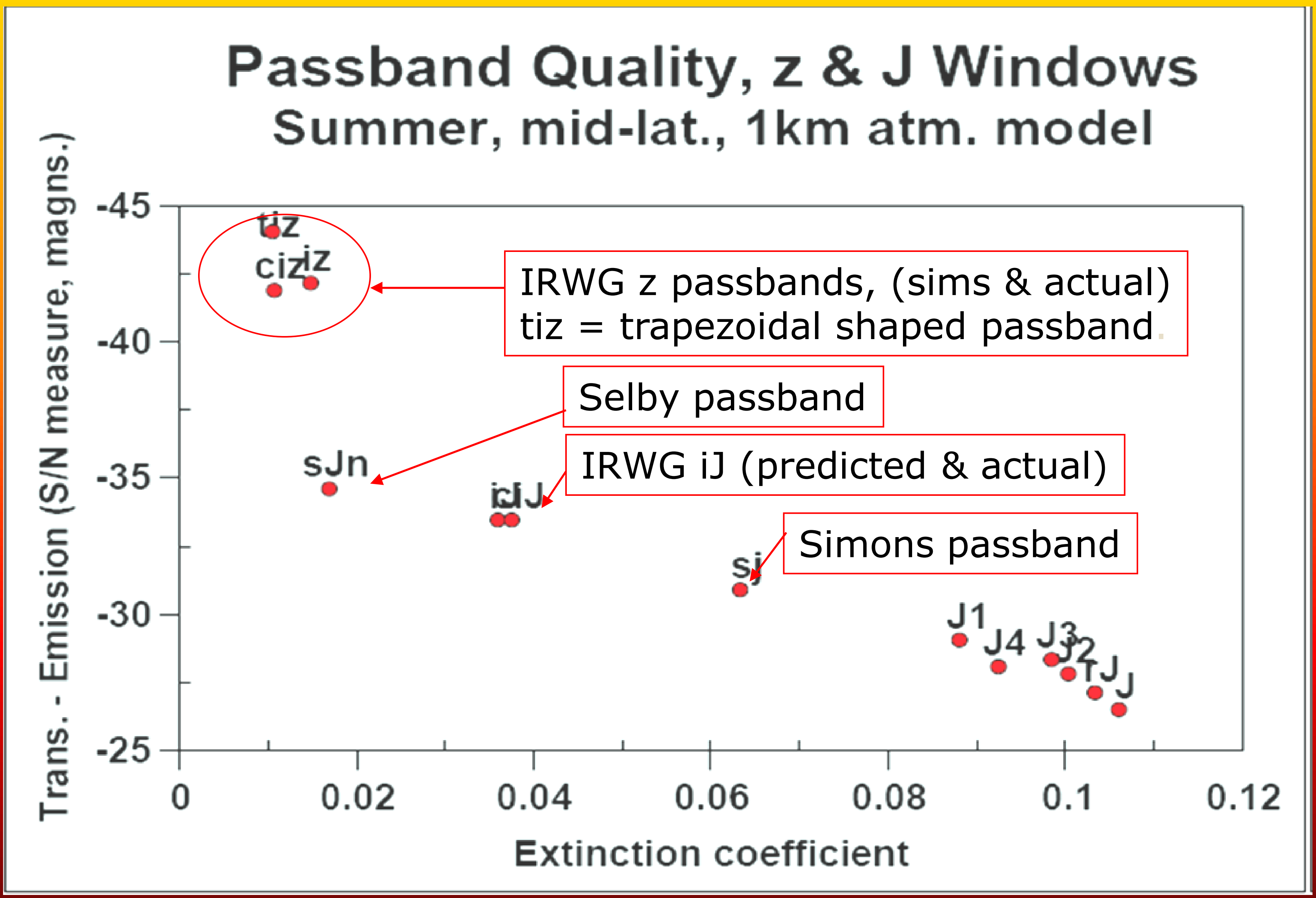

IR Photometry at all Photometric Sites

Bonus Benefits:

Near-IR IRWG photometry possible at both high and low elevation sites (if precise visual photometry already done there) --- but photometry done at high & dry sites can benefit from improved accuracy and transformability

If they are made widely available, they will be used!

- Automated IR systems with these passbands could establish a post-Johnson system more widely, creating a larger body of data to which future observations will be more fully transformable.

More purchases ➔ cheaper to purchase

Near-IR IRWG Passbands & Windows

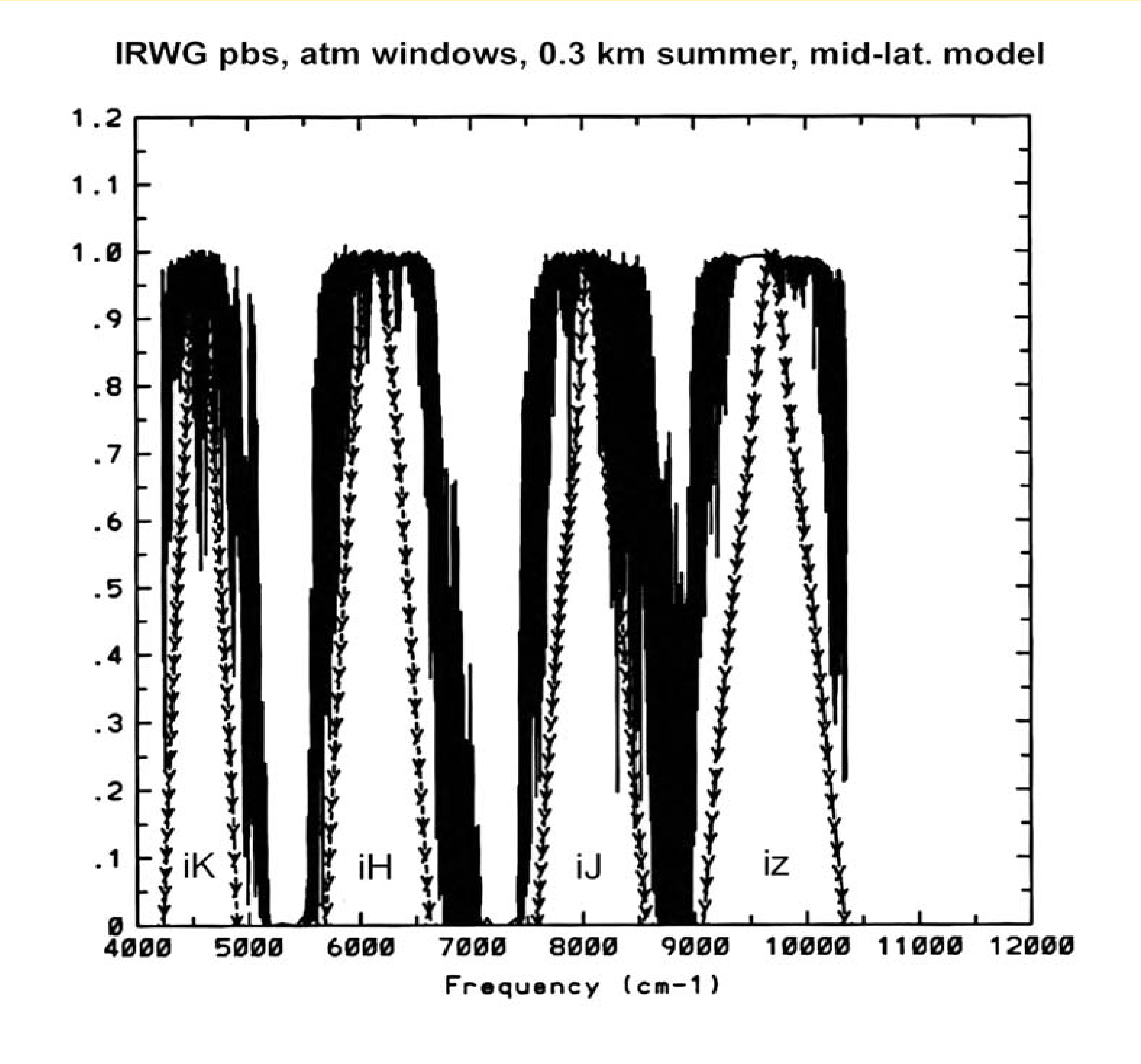

Overcoming Impediments

Impediments to IRWG use are not severe:

- SNR varies inversely with both extinction and with a measure of the Forbes effect. Therefore,

  small loss of raw throughput is recouped in signal-to-noise gain.

- Reduced costs can be realized through bulk orders with uniform filter specifications.

To be used more widely at IR observatories:

We encourage use to build a large body of observed data and enlarge the list of standards.

IRWG iz passband extinction curves

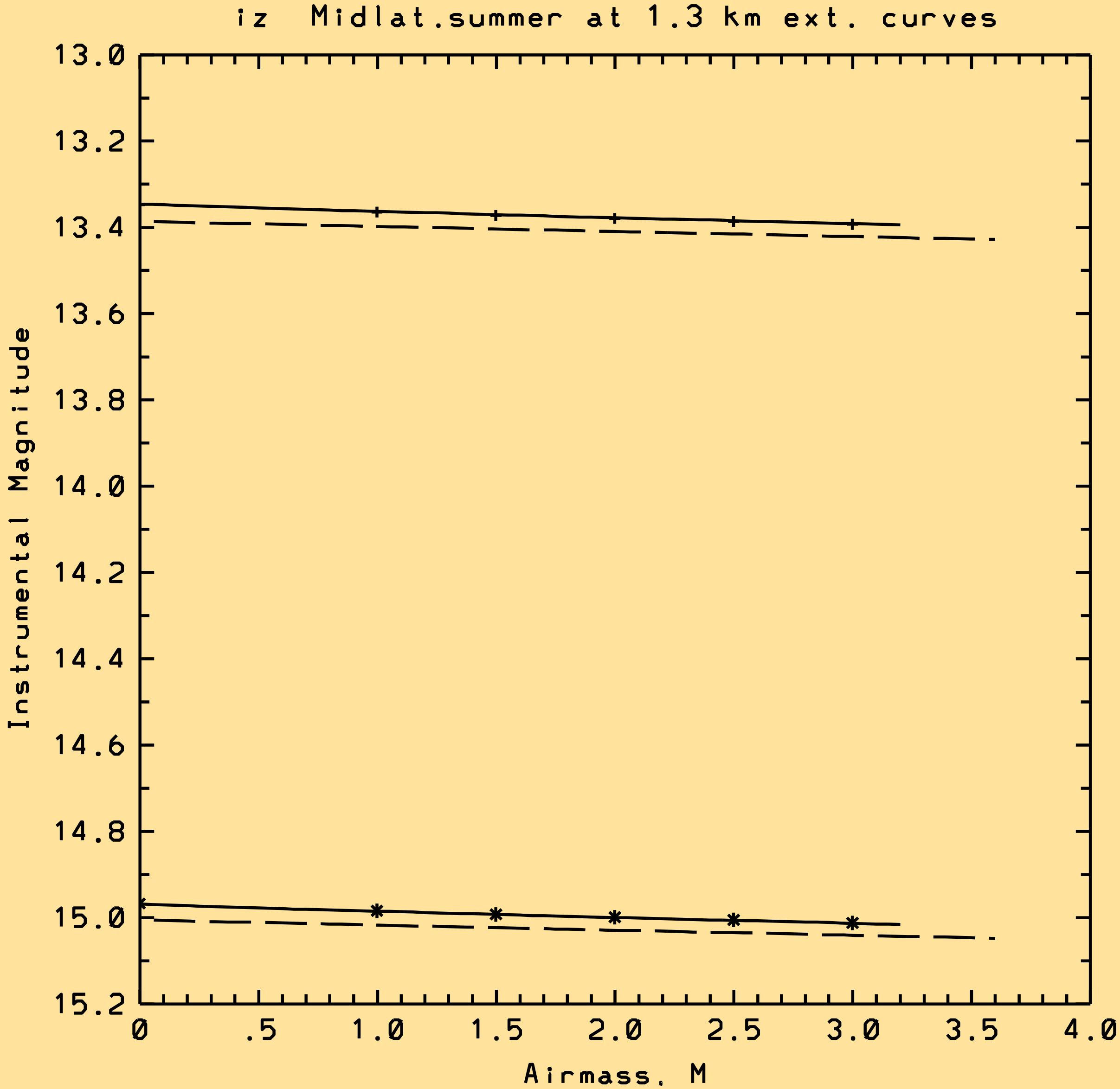

Figures of (De)Merit for Z, J window Passbands

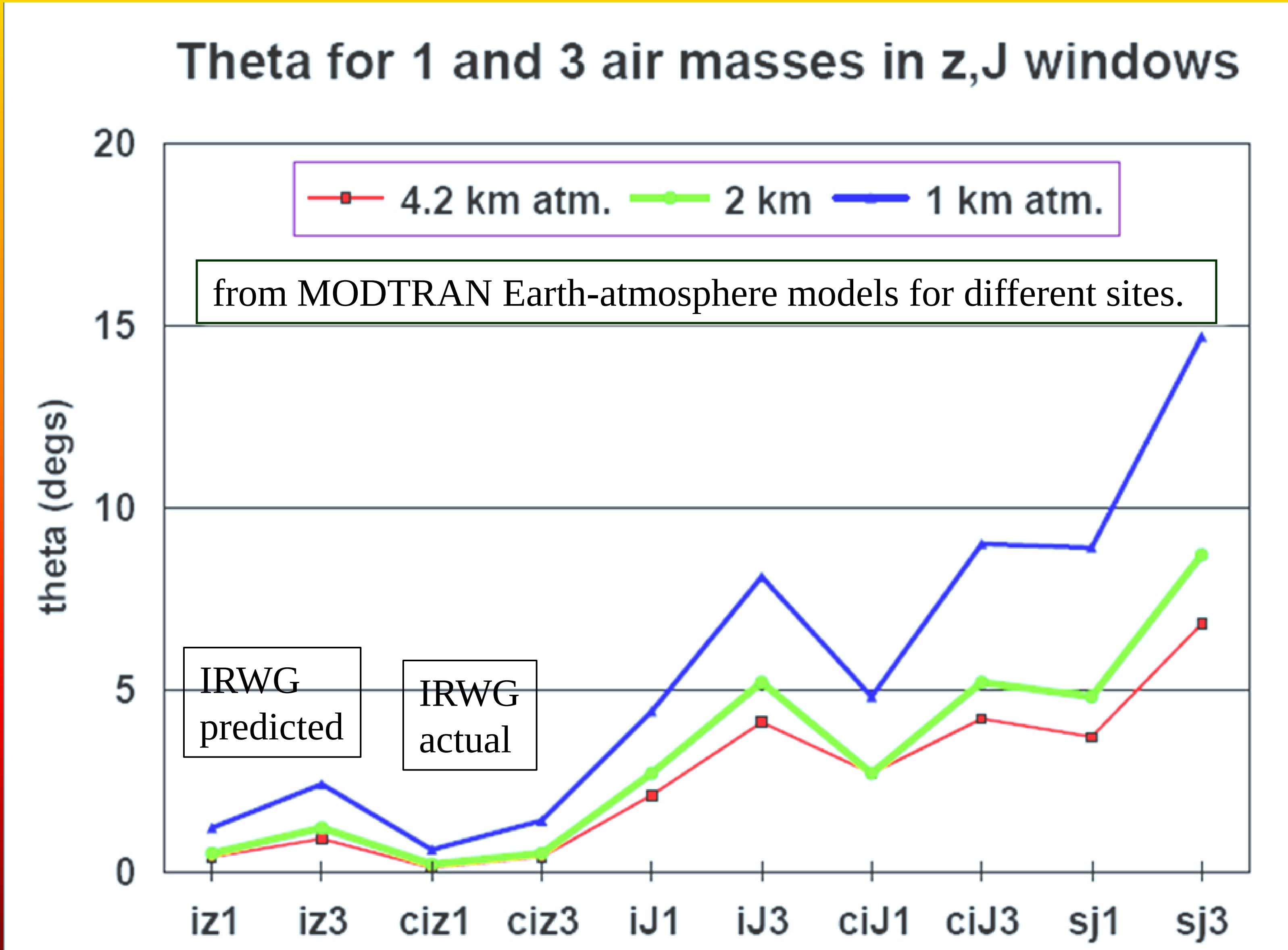

theta: measure of distortion in spectral flux from atm. absorbers

Johnson "H" passband Extinction Curves

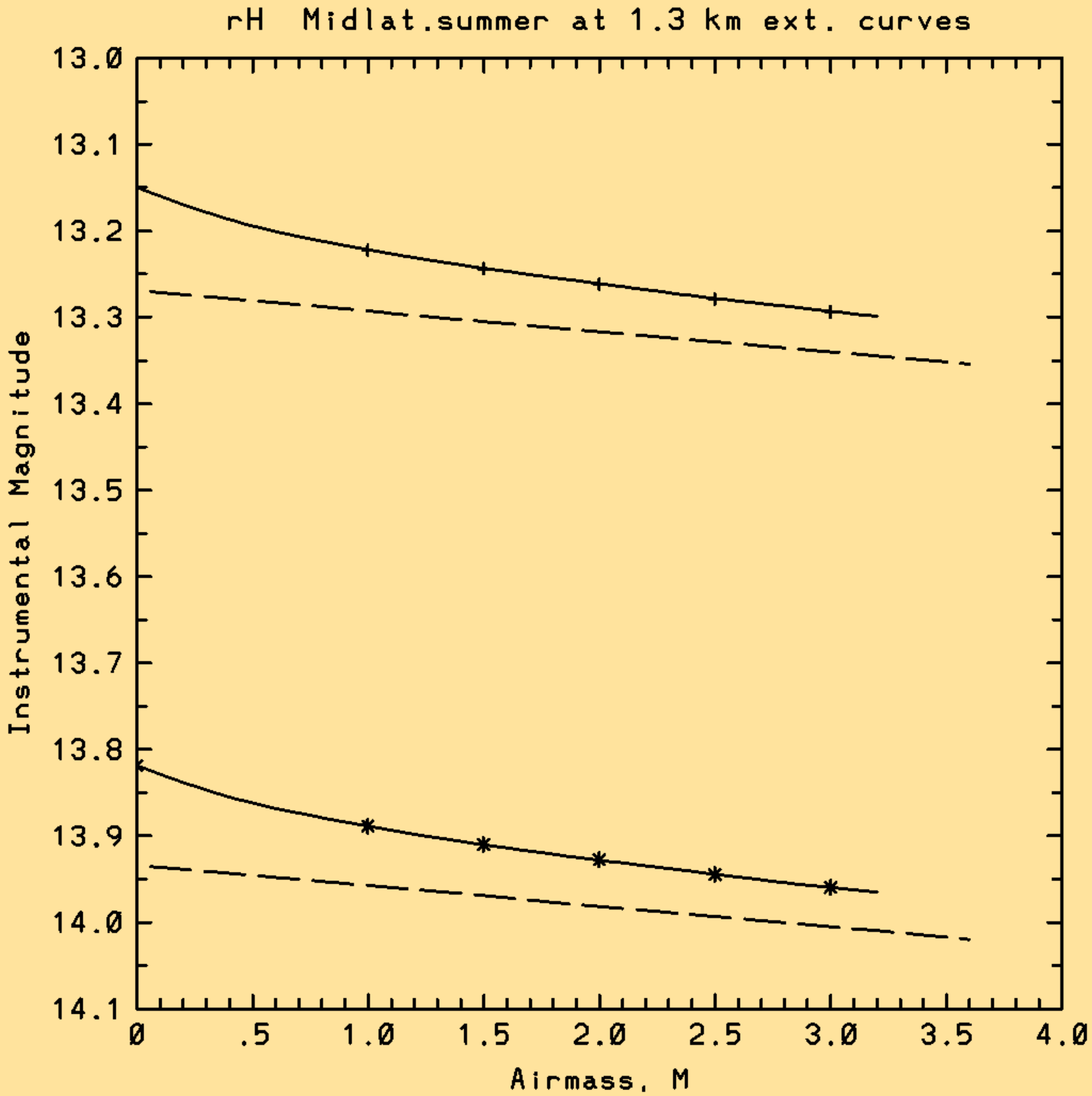

IRWG iH passband Extinction curves

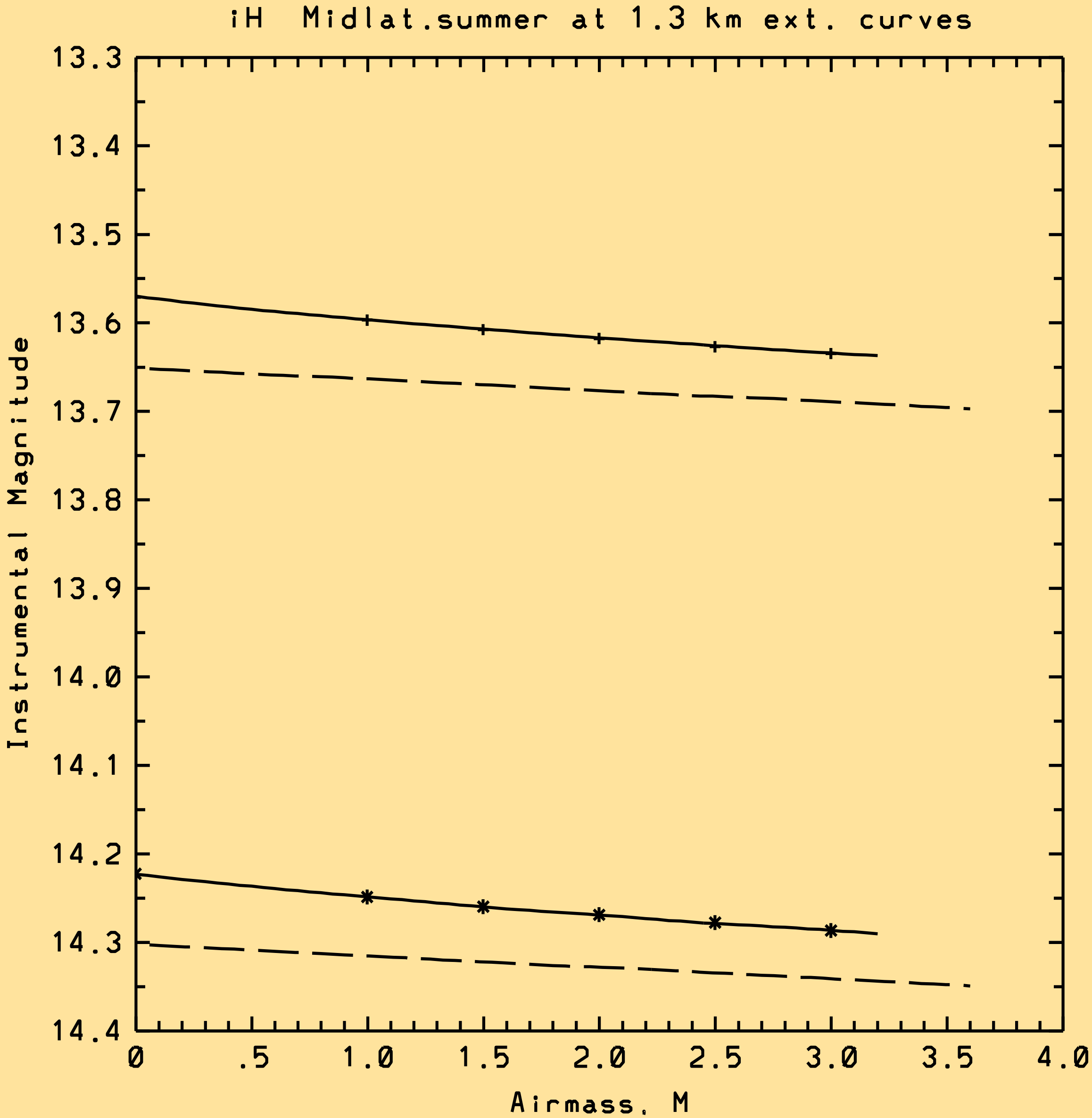

Theta, Forbes effect, and SNR for H Window PBs

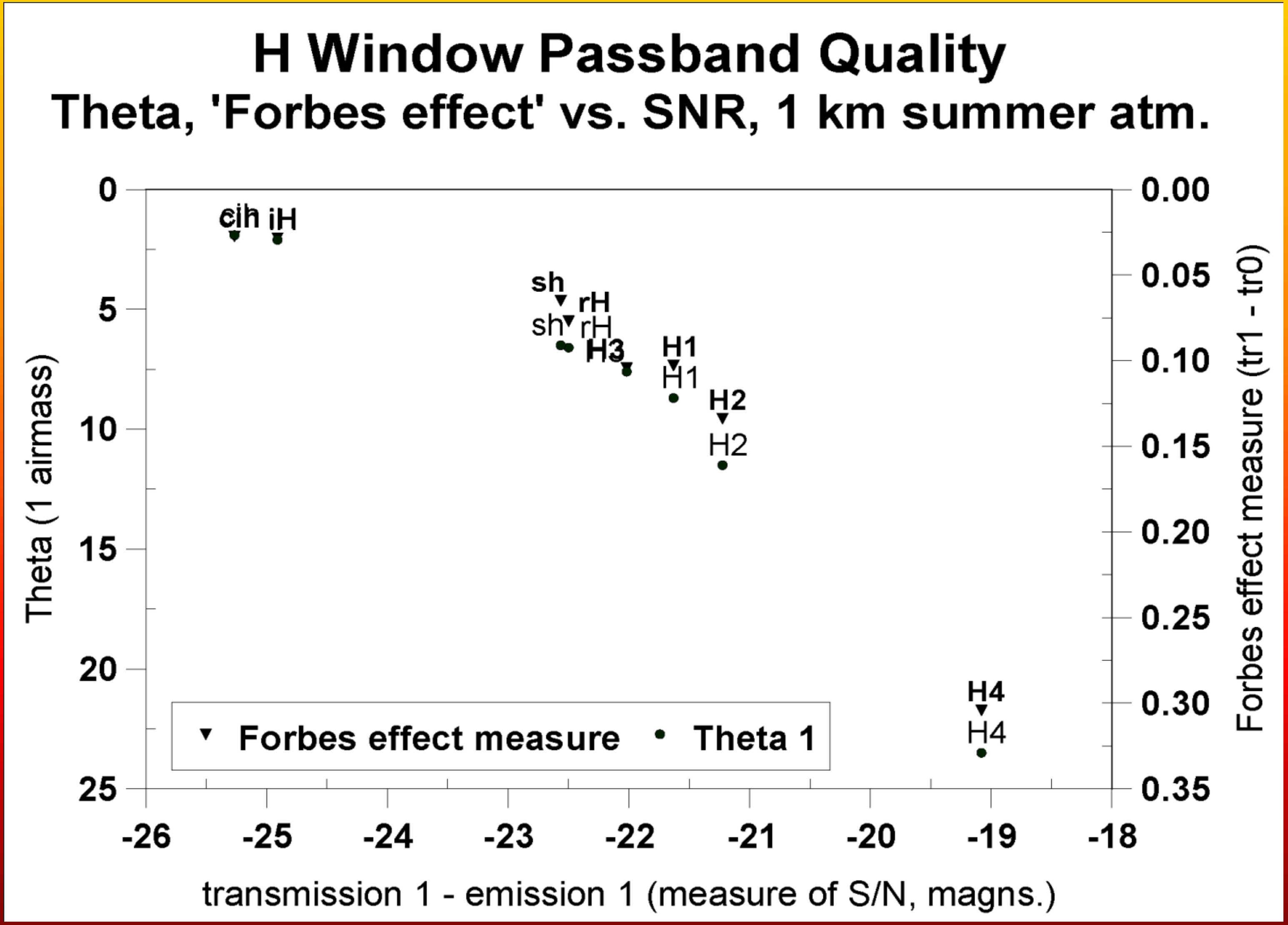

K Window and Passbands

Mid-latitude, 1.8-km elevation MODTRAN 3.7 atmospheric model

Legend:
K = Johnson pb
r = newer version
i = IRWG iK pb
c = Custom Scientific Corp fabrication of iK
s = Simon’s short and long K passbands

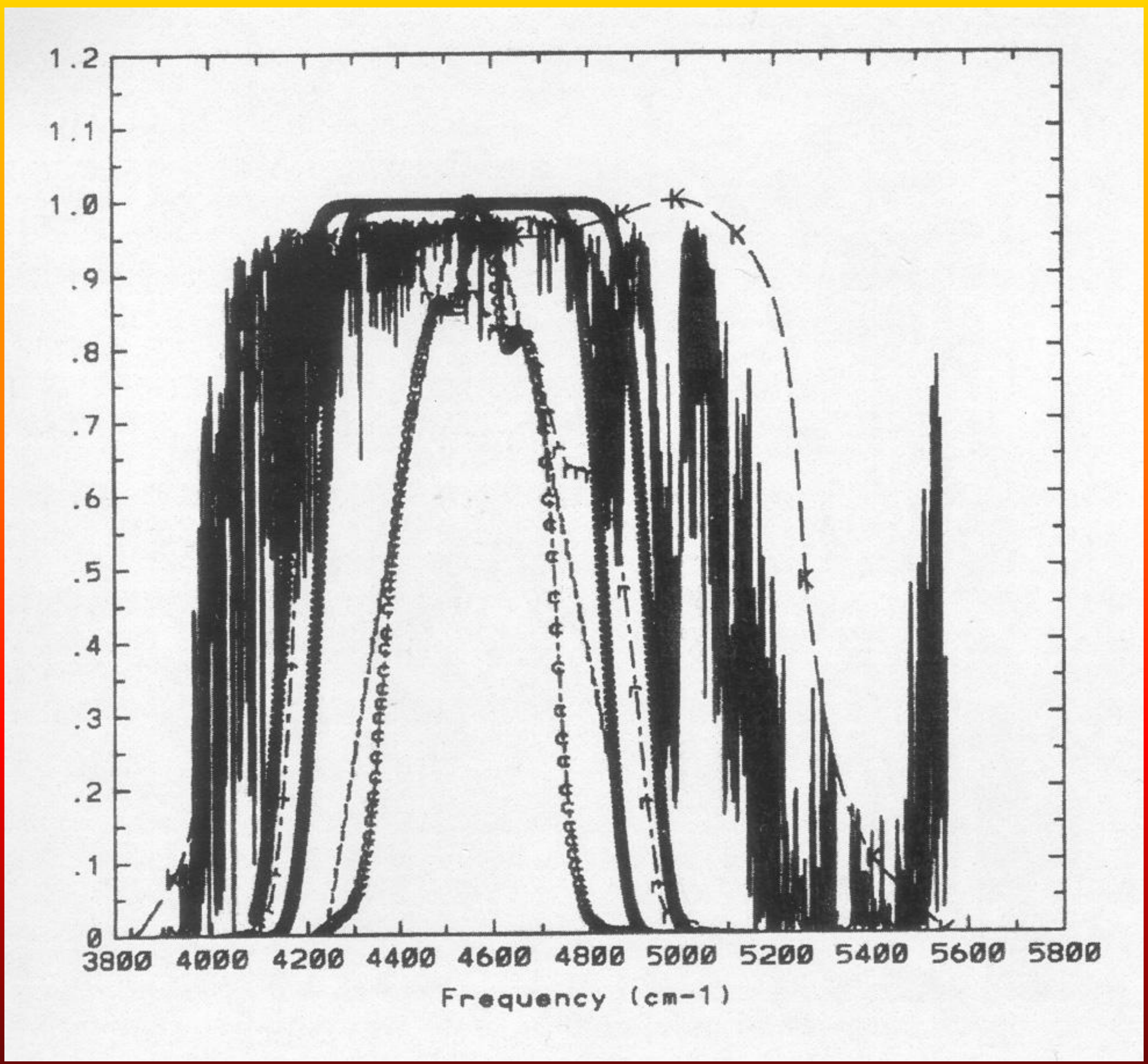

Modern Johnson short-K passband Extinction Curves

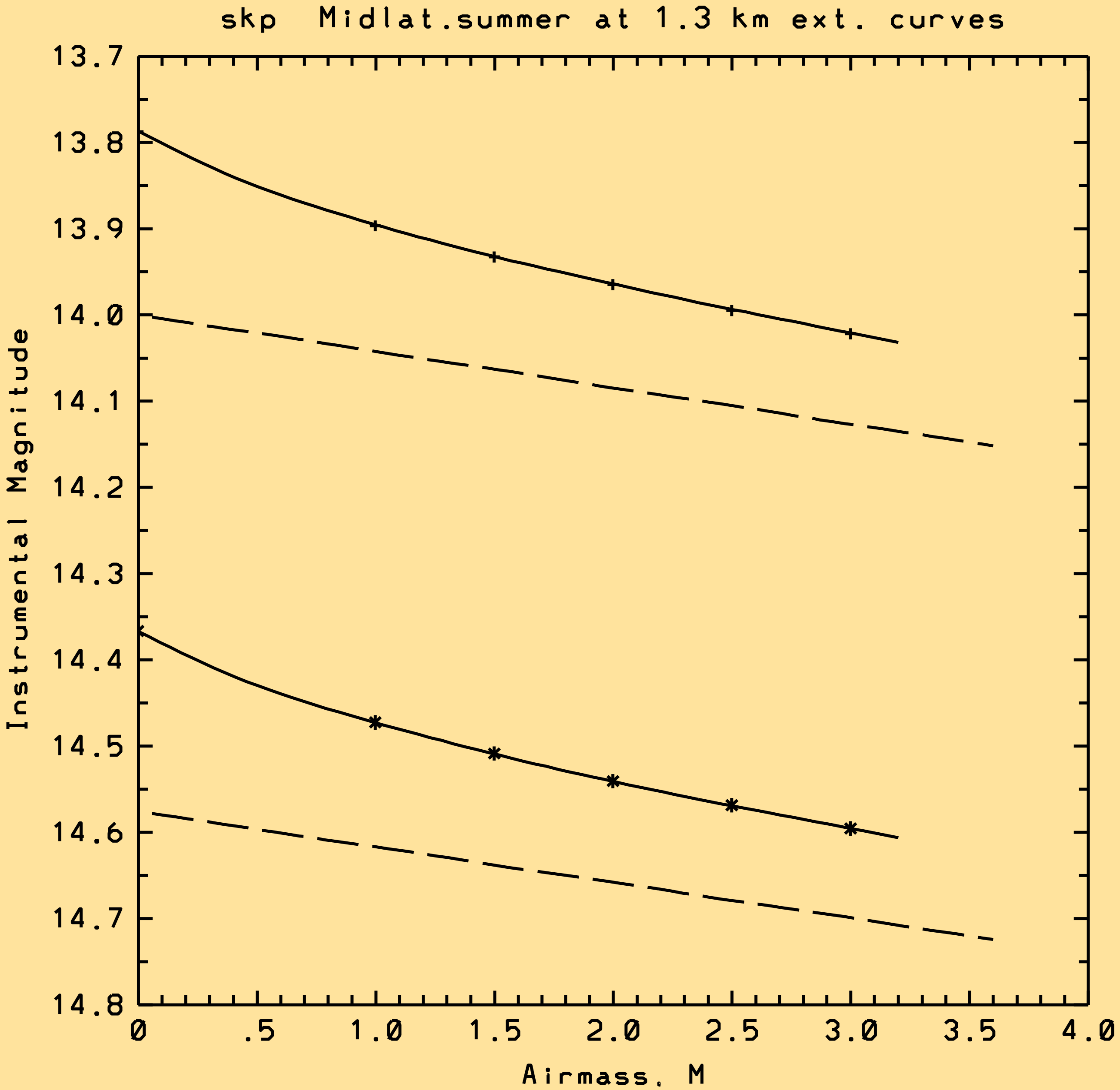

IRWG iK Passband Extinction Curves for same site

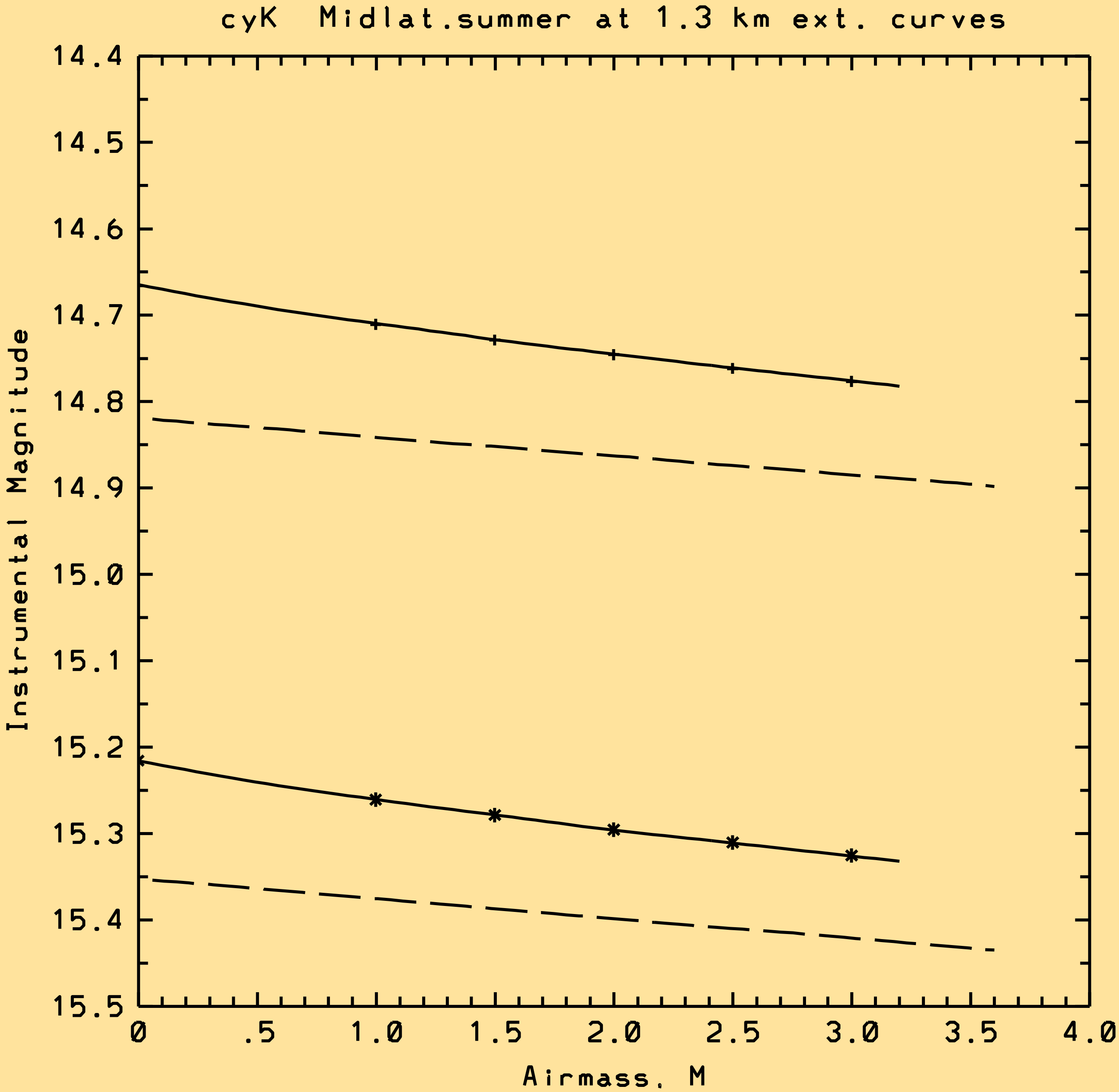

How do the simulations compare to real data?

Extinction in the IRWG-near-IR passbands: data from the ARCT at the RAO

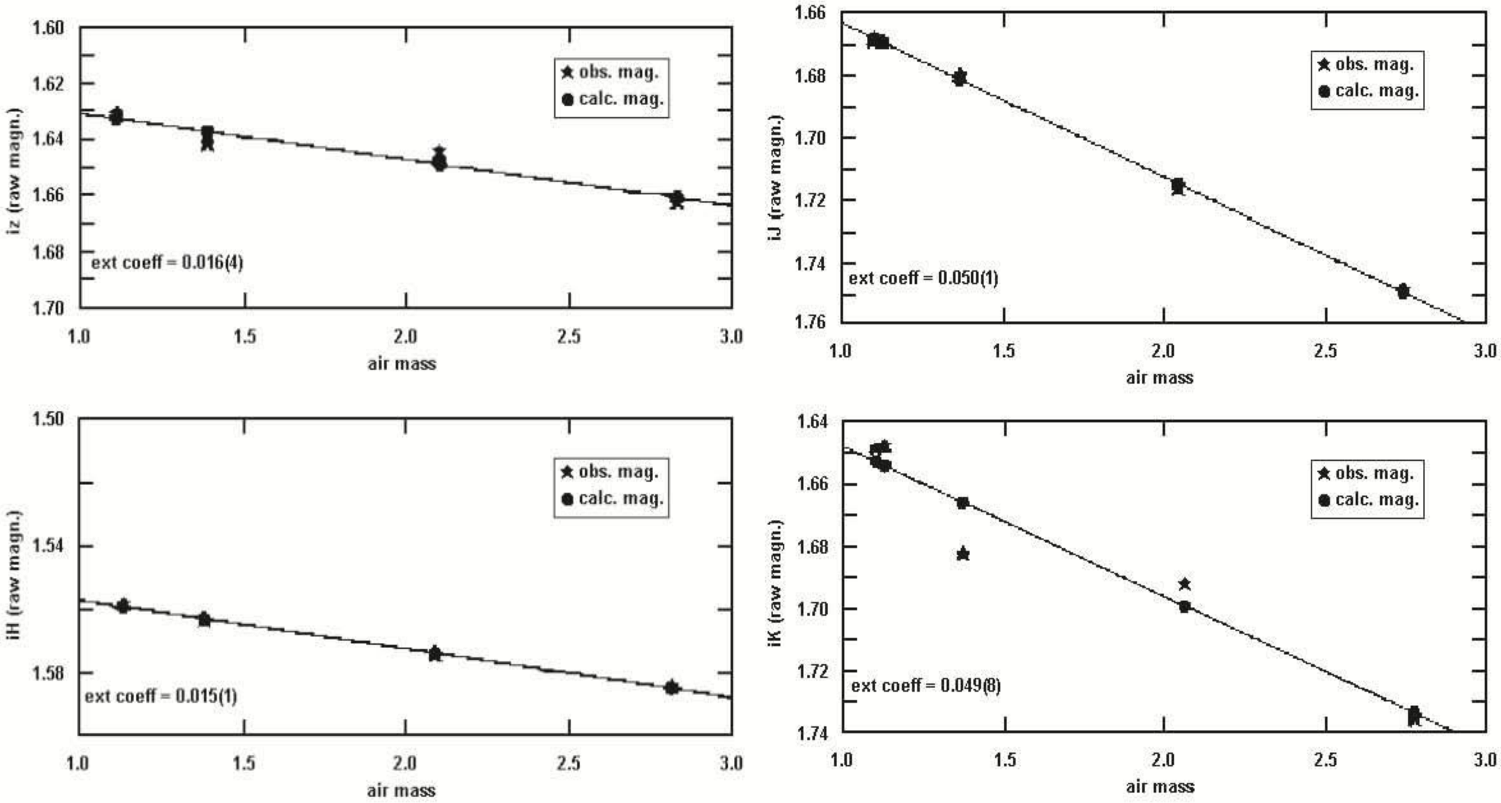

Figure 7. Observed extinction plots for the night of Sept. 26, 2000, for the IRWG passbands, made on the RAO's 1.8-m ARCT. Linear fitting to the data may be extrapolated to give a close approximation to outside-the-atmosphere magnitudes. The extinction star was Vega. The derived linear extinction coefficients and their uncertainties, in units of the last decimal place (in parentheses) are given in the lower left corners of the plots, viz., about 0.02, 0.05, 0.02, and 0.05 magn./airmass for the *iz, iJ, iH,* and *iK* passbands, respectively.

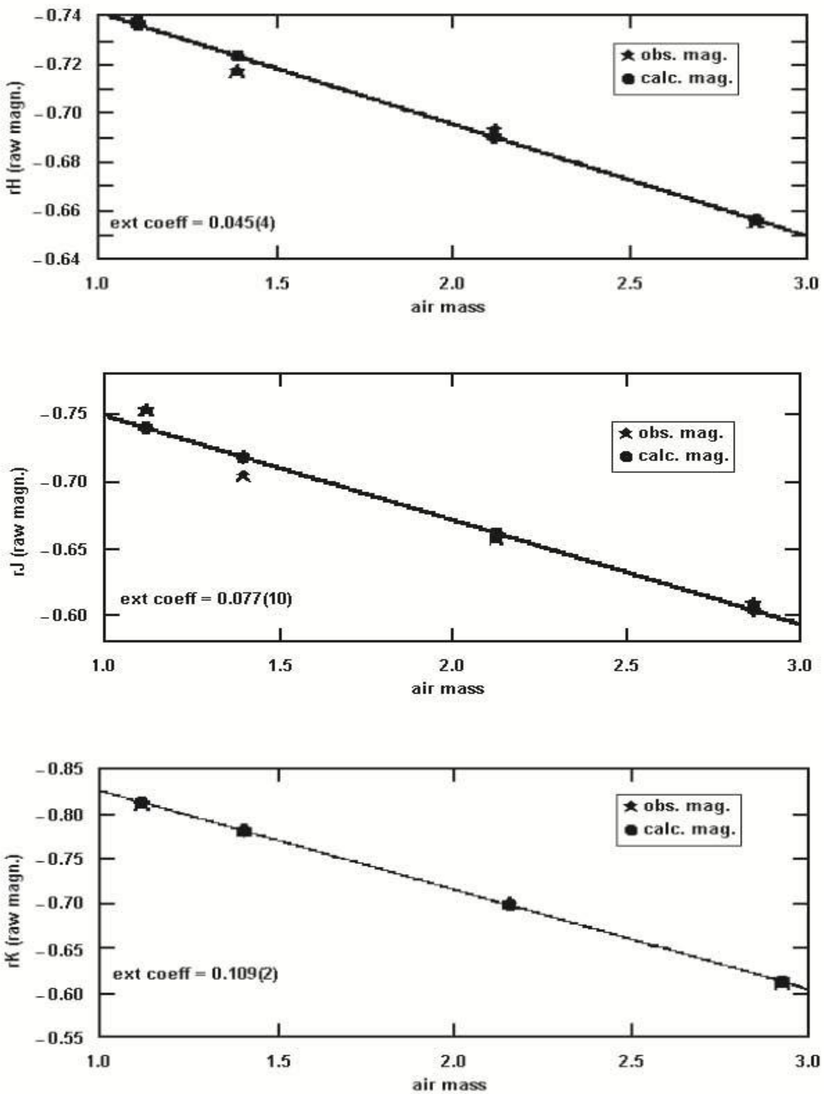

Figure 8. Observed extinction plots for the same night in which the IRWG passbands were used, and for the same extinction star, Vega, but obtained with an older set of passbands. The derived linear extinction coefficients and their uncertainties are again indicated. Note that they are systematically higher than for the IRWG passbands, about 0.05, 0.08, and 0.11 magn./airmass for the *rH*, *rJ*, and *rK* passbands, respectively.

Extinction results from same night as the previous slide, but through older "Johnson" JHK passbands. Note the larger coefficients: **0.08**, **0.05**, **0.11** mags/airmass for the **rJ**, **rH**, and **rK** passbands. (The IRWG passdbands gave: **.02**, **.05**, **.02**, and **.05** for the **iz**, **iJ**, **iH**, and **iK** passbands, resp.)
The RAO is located at 51deg N and at an elevation of 1.3 km.

Near-IR Passbands Summary

- All Johnson IR passbands suffer from effects of water vapor absorption

  → Non-linear extrapolation to 0 AM needed (Forbes effect)
- MKO-NIR and IRWG passbands reduce exposure to water vapor effects at MKO; at lower elevation sites, IRWG pbs are more effective
- IRWG (Young et al. 1994; Milone & Young 2005)

  offer improved SNR, extinction, & transformation from different altitude sites

  But we can also mention the longer passbands …

L-Passbands

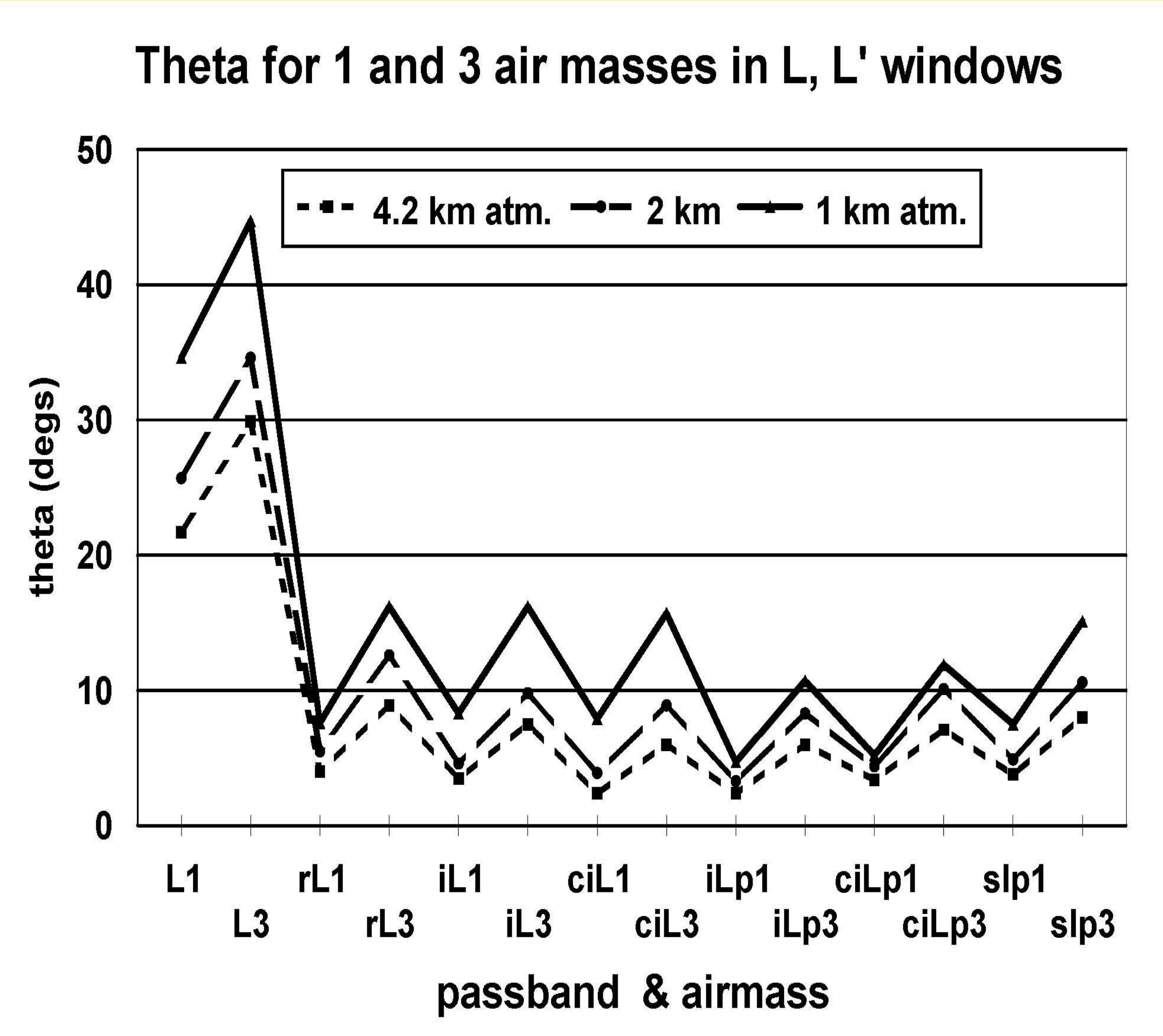

Theta for 1 and 3 air masses in L, L' windows
4.2 km atm.
2 km
1 km atm.
theta (degs)
50
40
30
20
10
0
L1
L3
rL1
rL3
iL1
iL3
ciL1
ciL3
iLp1
iLp3
ciLp1
ciLp3
slp1
slp3
passband & airmass

M Atmospheric Window, 4.2 km site

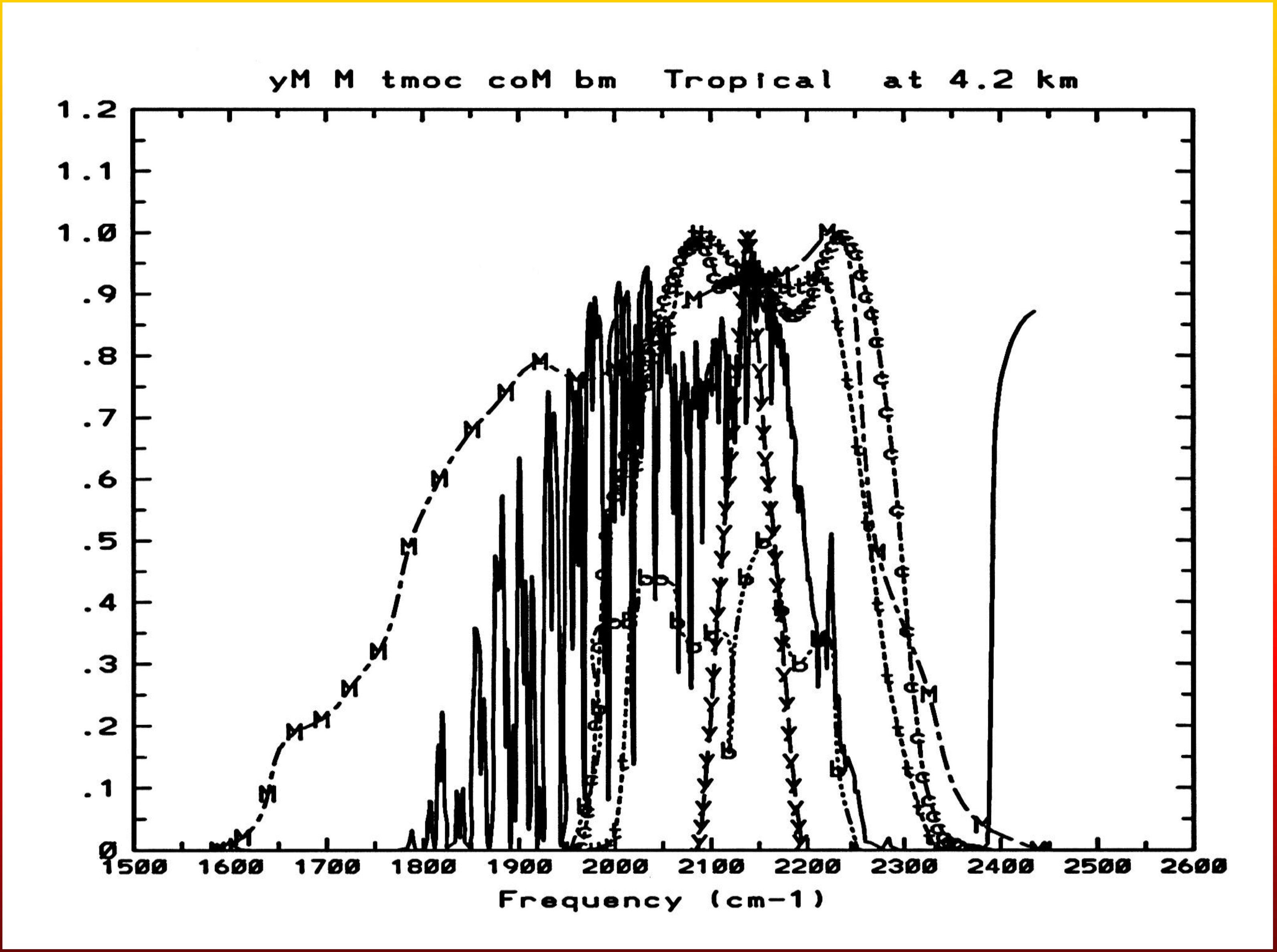

Johnson M passband extinction, 4.2 km site

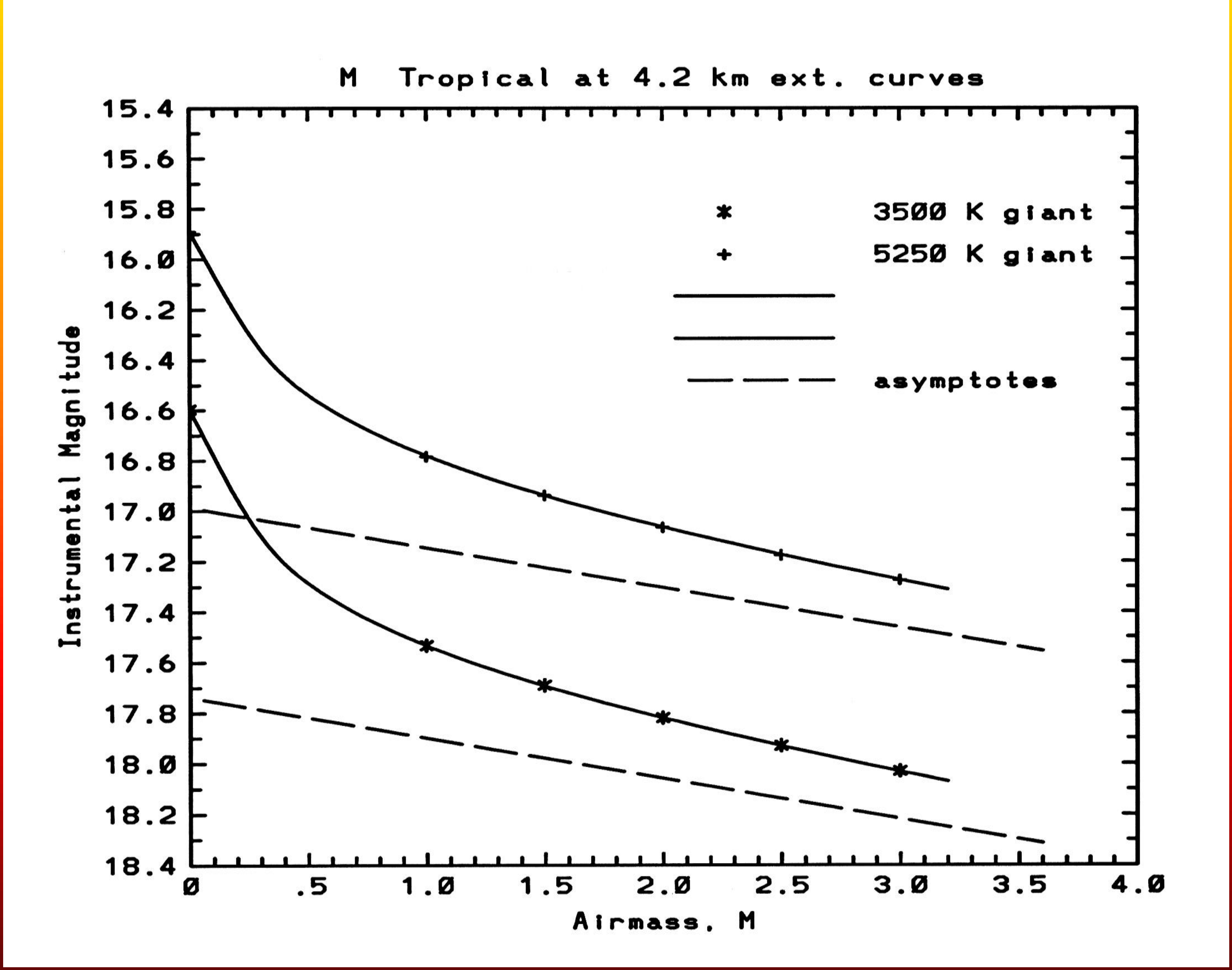

IRWG iM passband extinction, 4.2 km site

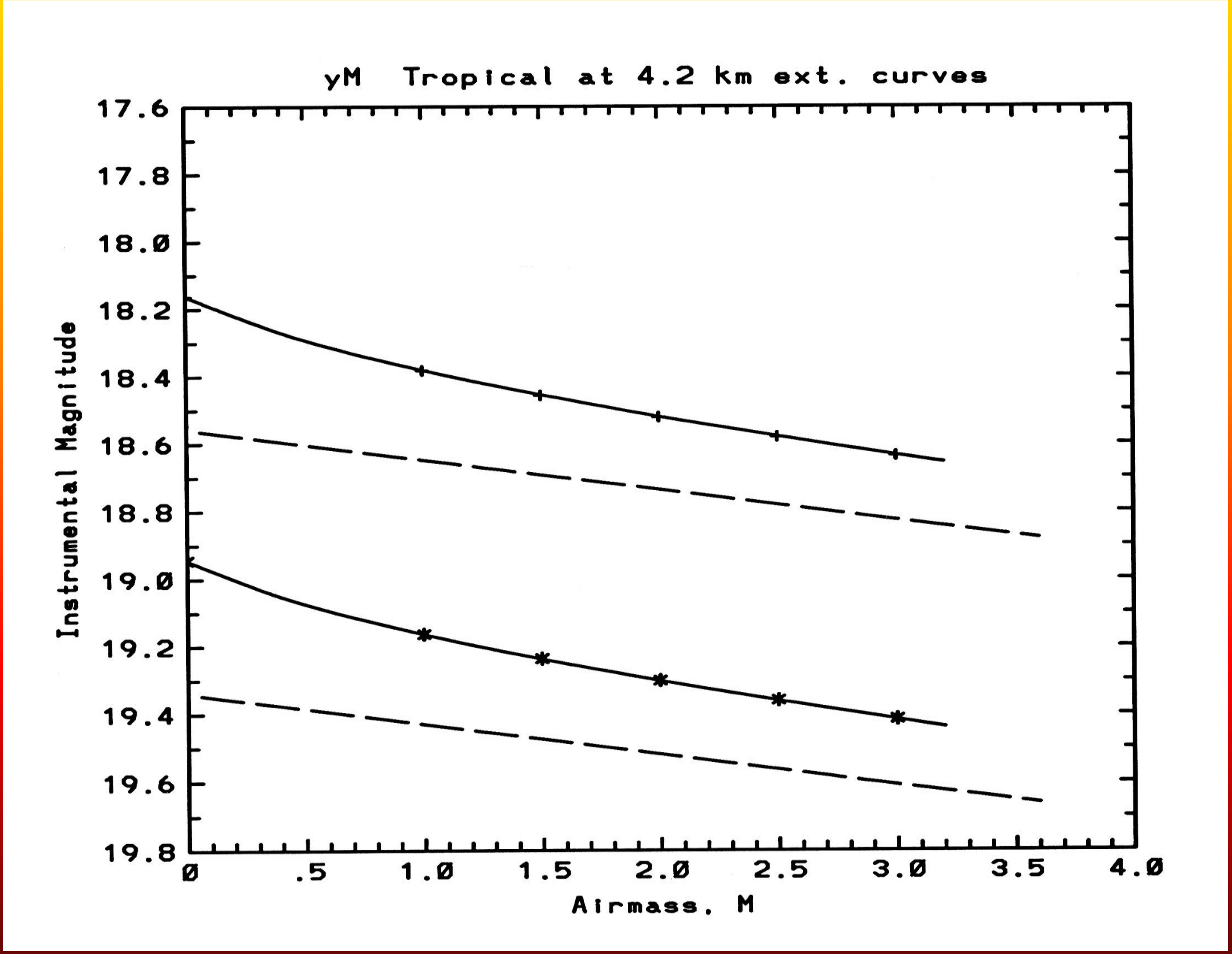

M Atmospheric Window, 2 Km site

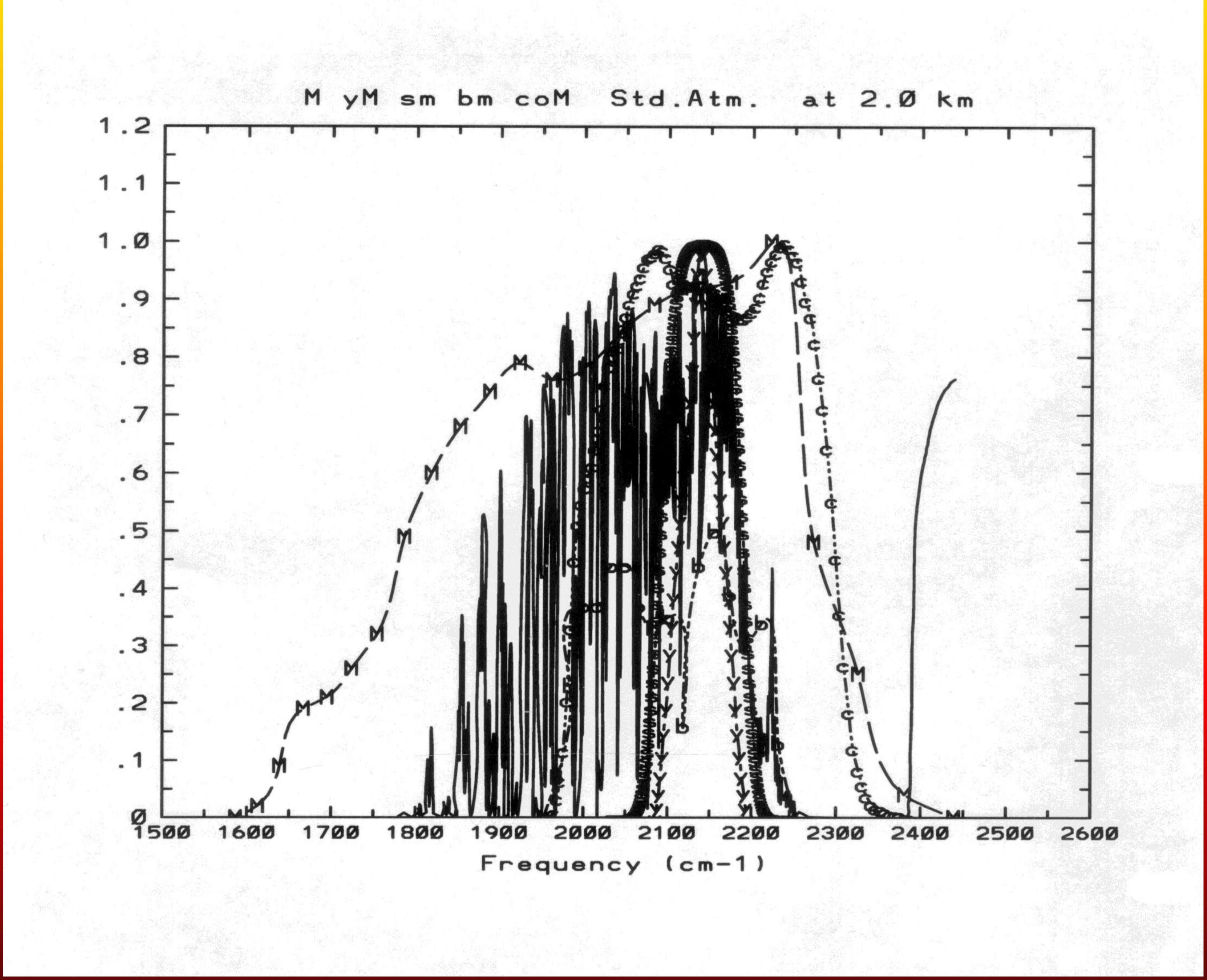

IRWG iM passband extinction for RAO

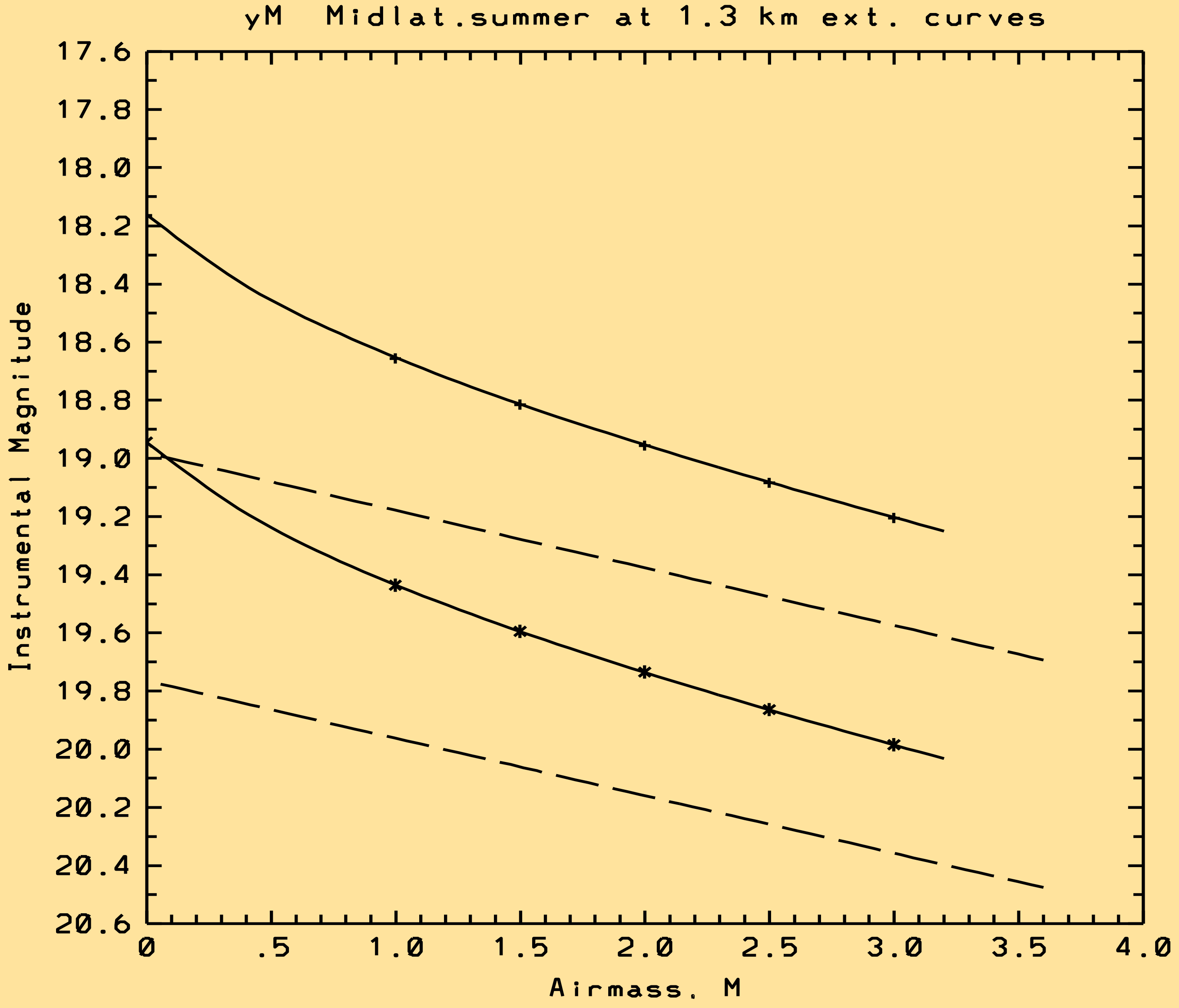

N Atmospheric Window, 4.2km site

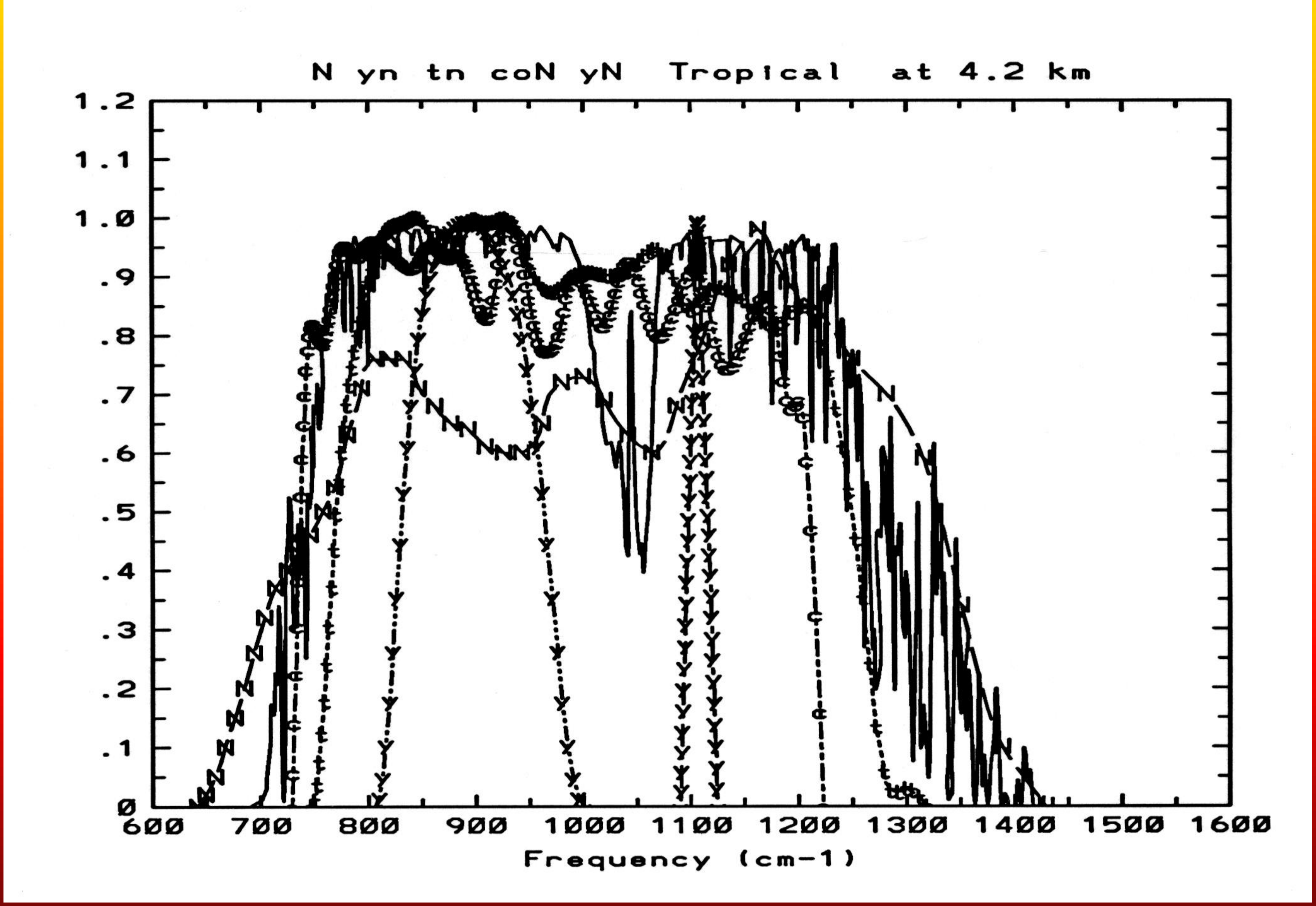

Johnson N Passband extinction, 4.2km site

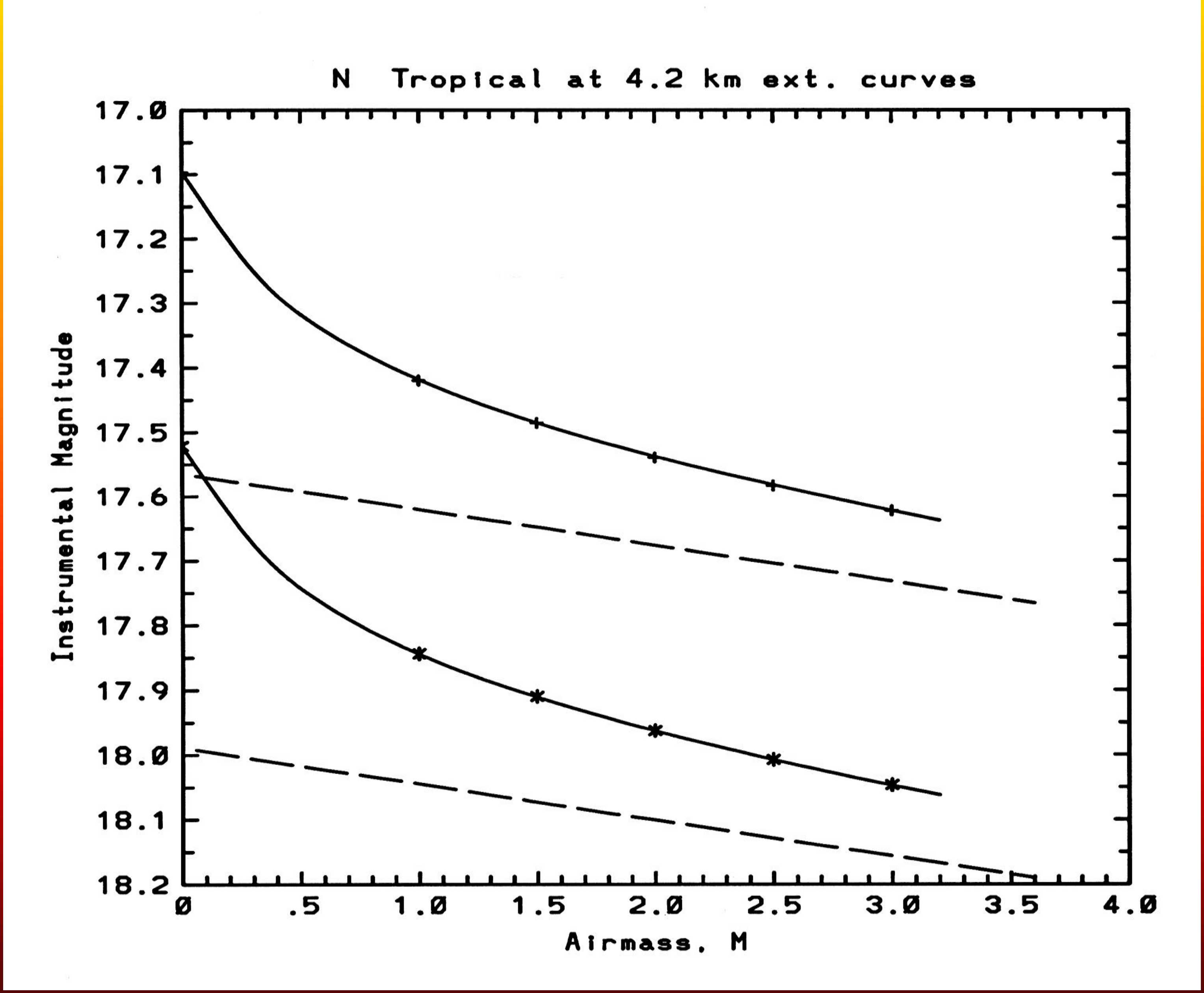

IRWG iN Extinction, 4.2km site

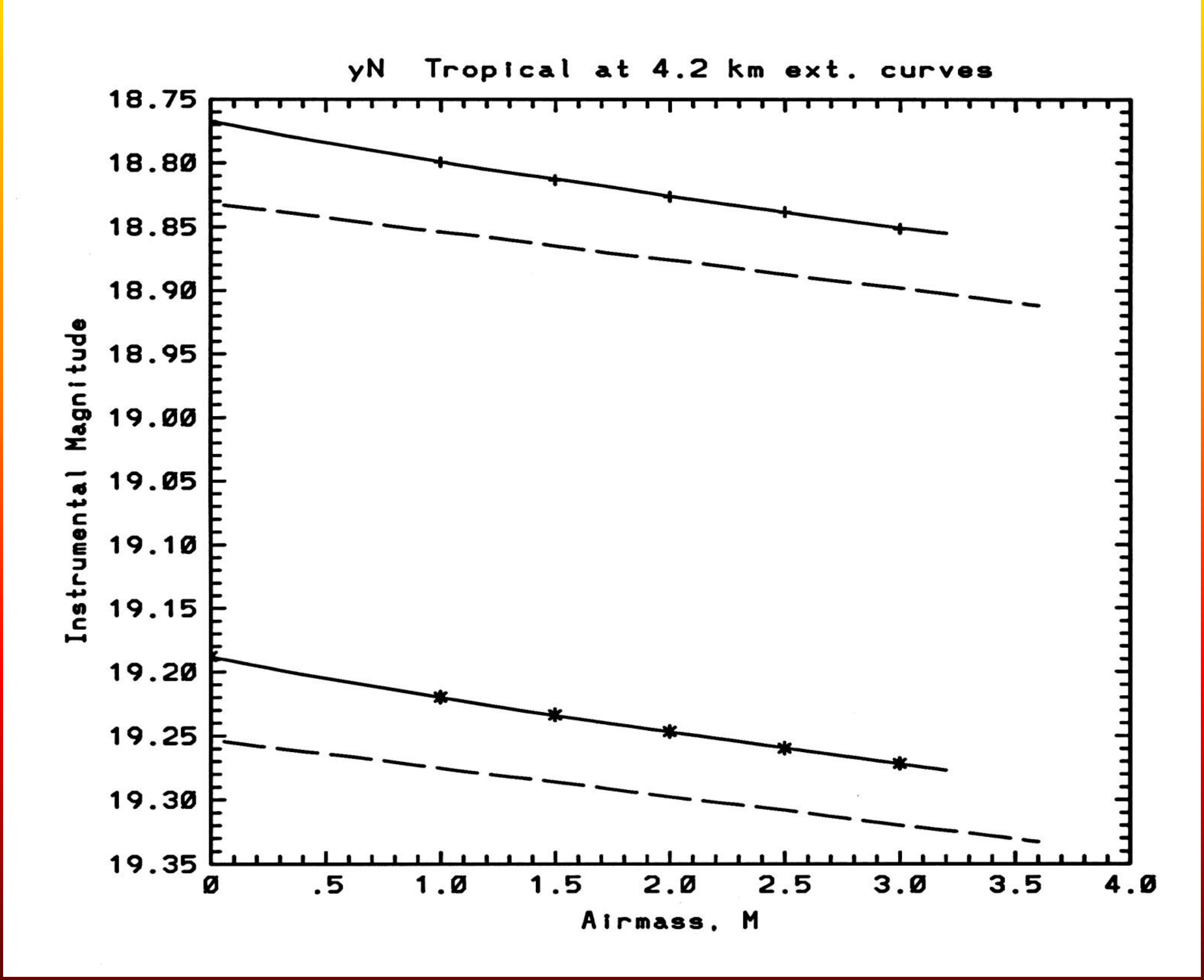

Johnson N passband extinction, 1.3km site

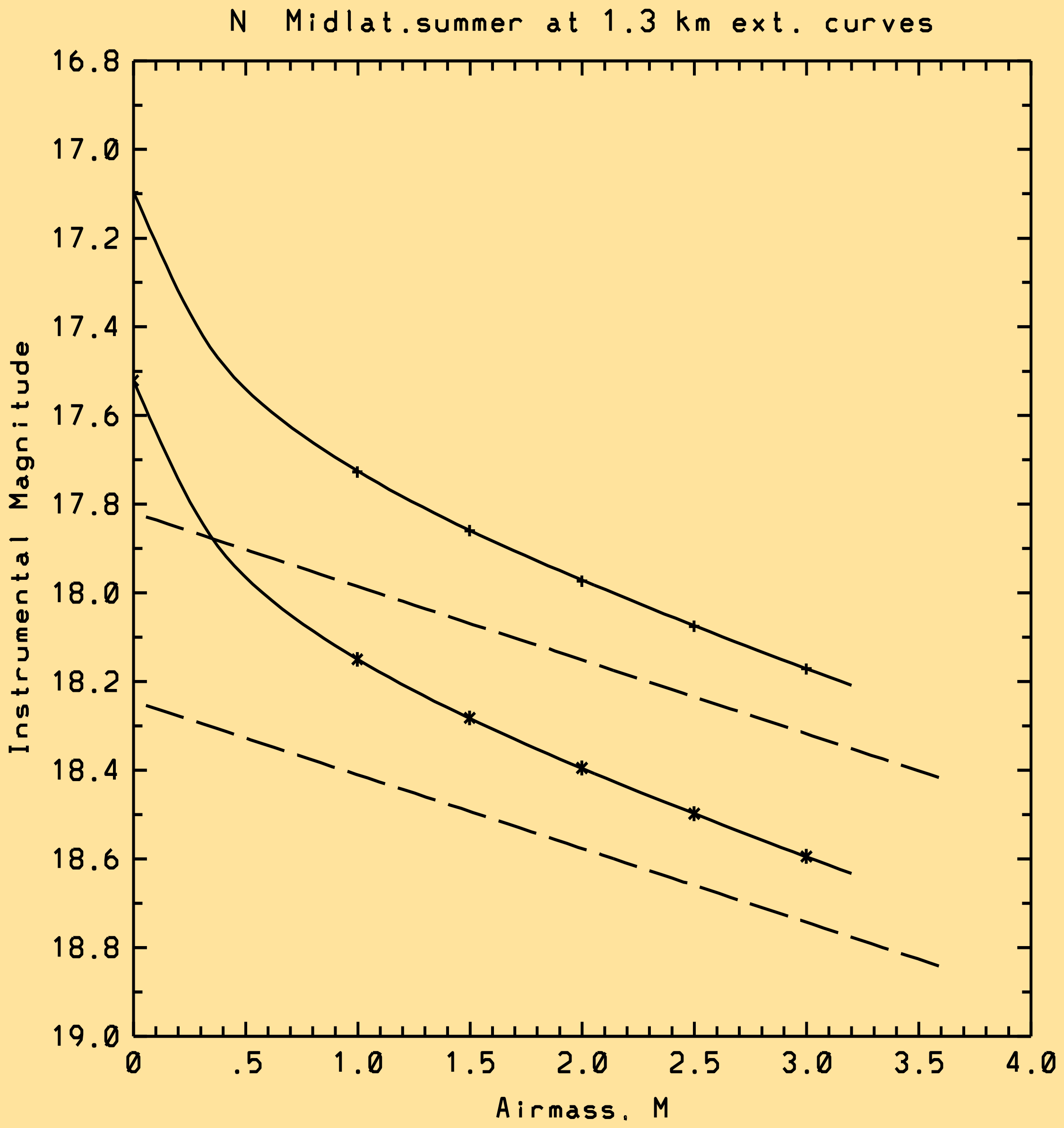

IRWG iN Extinction, 1km site

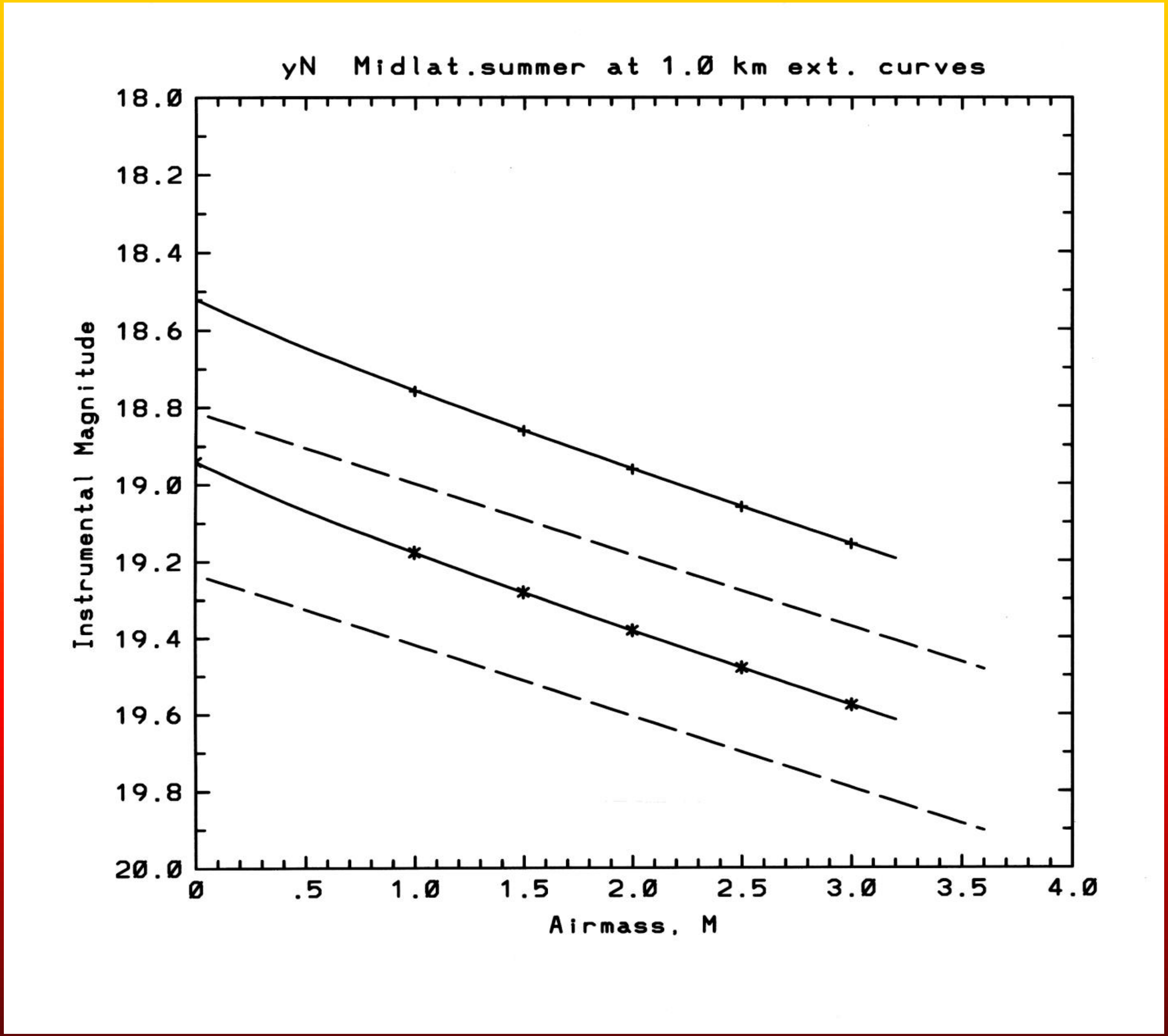

IRWG in passband extinction for 1.3km site

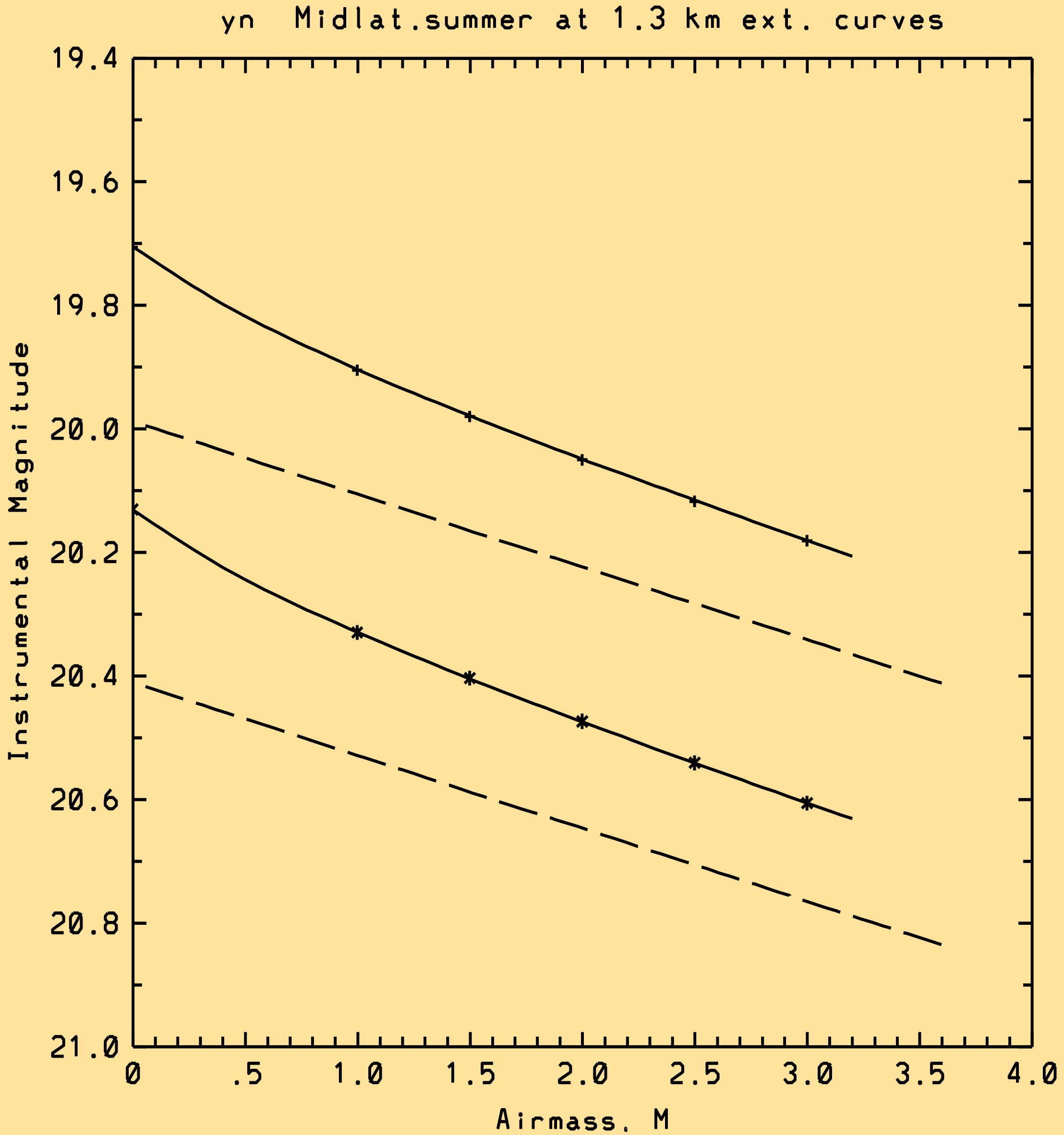

Future of IRWG Work

- Improved light curve precision to support
  - Improved analysis precision and accuracy
- Treatment of aerosol extinction
- Real-time monitoring of IR extinction

BUT, these depend on the work of the IRWG:

So, join today!

Contact: milone@ucalgary.ca

Refs to IRWG passband work

- Young, A.T. (1989) in Milone *Infrared Extinction and Standardization* (Springer) , 6
- Young, A.T., Milone, E.F., & Stagg, C.R. 1994, *A&AS*, **105**, 259
- Milone, E.F., Stagg, C.R., Young, A.T. (1995) in Bode Robotic Observatories (Wiley), 117
- Milone, E.F. & Young, A.T. 2005, *PASP*, **117**, 405
- Milone, E.F. & Young, A.T. 2007, in Sterken *The Future of Photometric*, *Spectrophotometric and Polarimetric Standardization*, ASP, **364**, 387
- Milone, E.F. & Young, A.T. 2008, *JAAVSO*, ***36***, *110*
- Milone, E.F. & Young, A.T. 2011, in Milone & Sterken, *Astronomical Photometry: Past, Present, & Future, in press*.

Acknowledgement

- This work has been supported in part by grants to EFM by the Canadian Natural Sciences and Engineering Council, the Physics & Astronomy Dept. of the University of Calgary, and the students of the Advanced Astrophysics Laboratory course who helped with observing, and the Infrared photometry community.
- We acknowledge also the assistance of the CFHT-AFAR LOC for support.

Additional Slides

- If time permits, ….

IR Photodiode Development --- practical for Z Window?

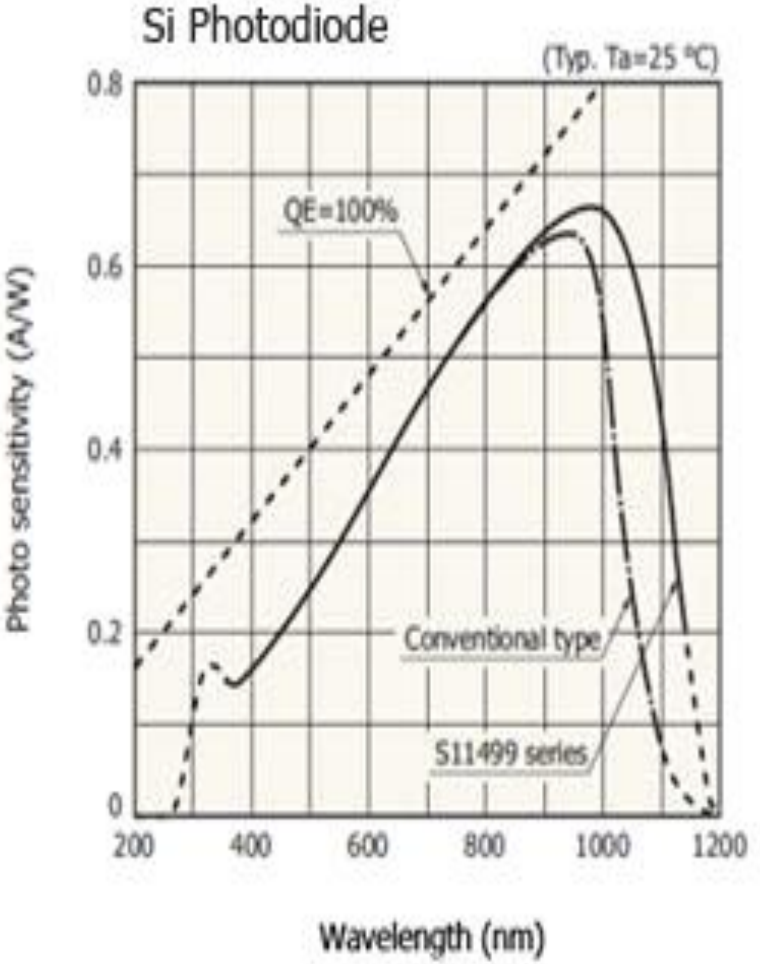

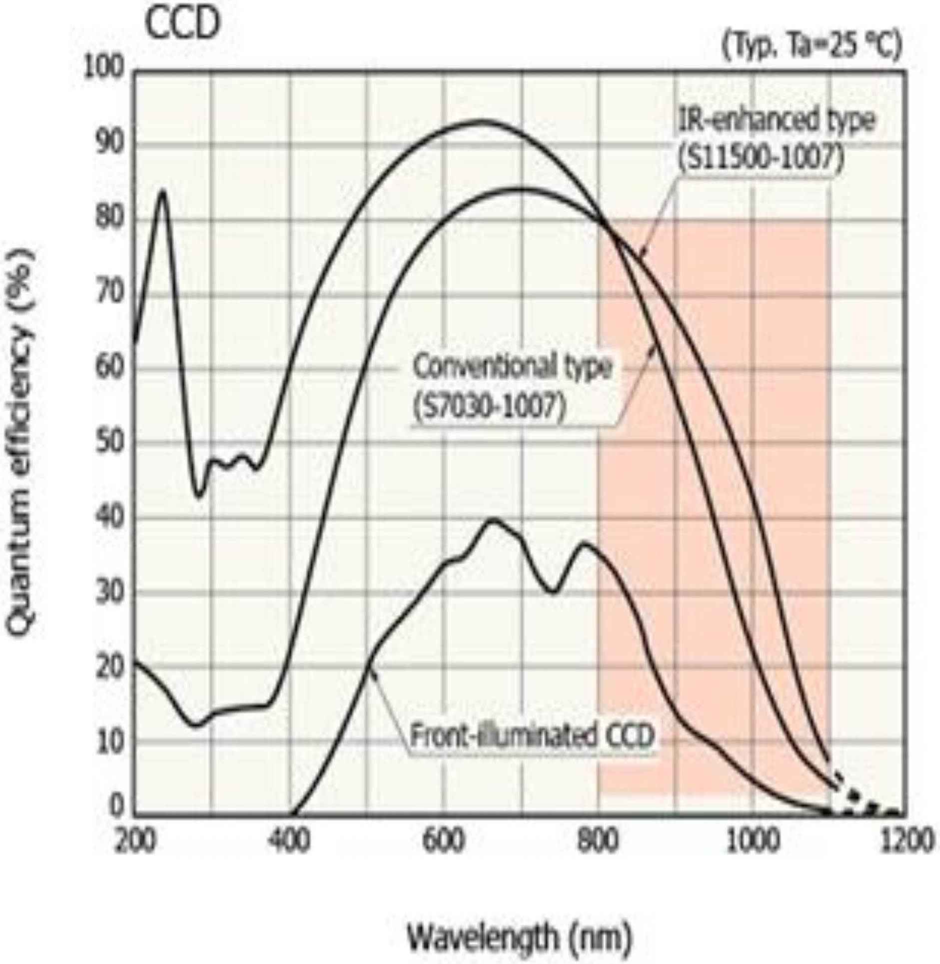

From Hamamatsu technical note on Photonics Spectra website

Problems with the 2002 Mass buy of MKO-NIR filters

- Designed for Gemini at Mauna Kea
- Fitted by eye to the window of Mauna Kea atmosphere → trans. problems with data from lower elevation sites
- Tight "roll-off" (<2.5%) → transformation problems from one filter batch to another.
- Interference filters have ripples, leaks, require frequent replacement [Solid-state etalons better?]

Optimizations of IRWG Passbands

Z Window

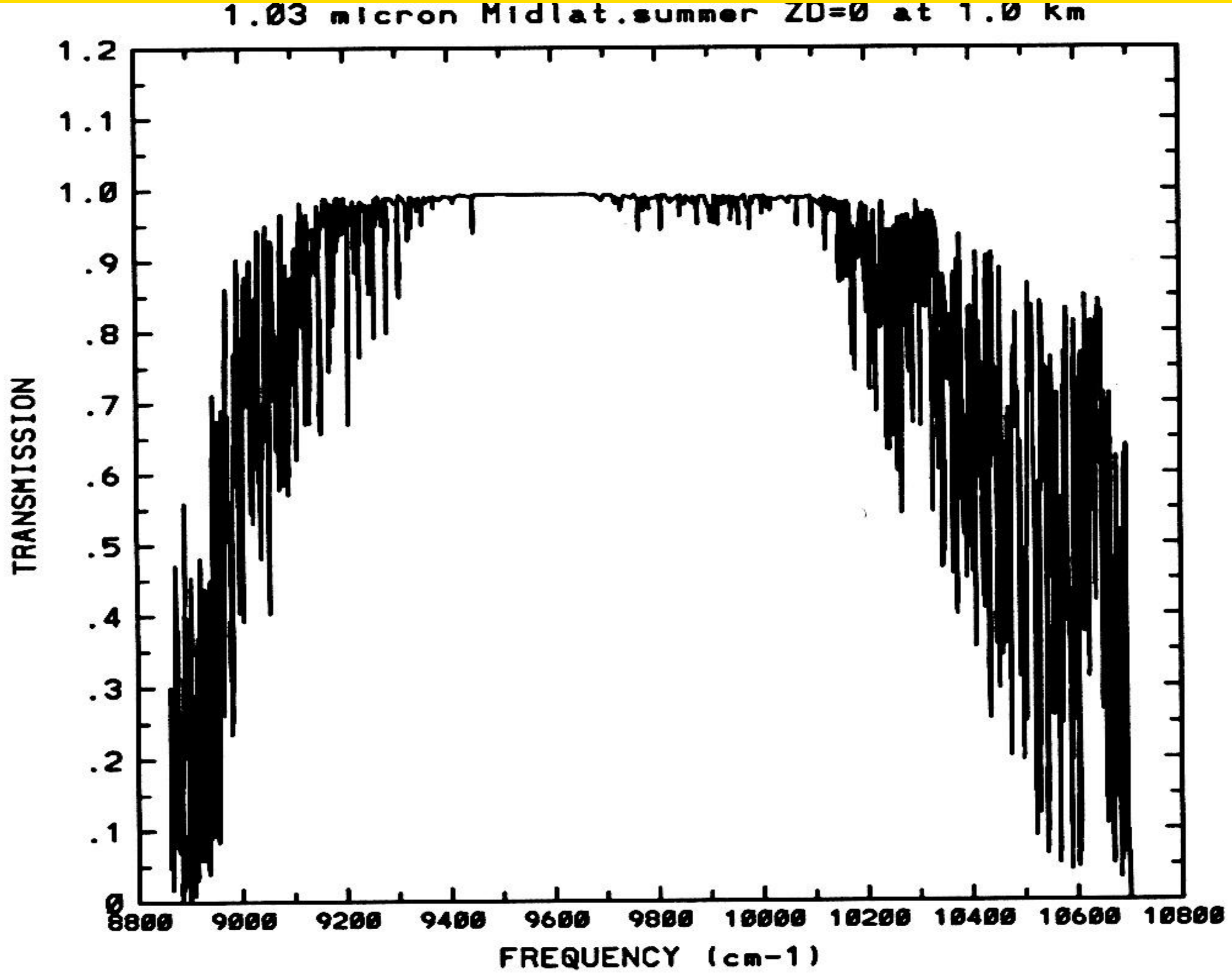

Fig. 8. The zenith transmission in the 1.03-micrometer window, for the mid-latitude summer atmosphere at 1 km above sea level.

Optimized passband for Z window

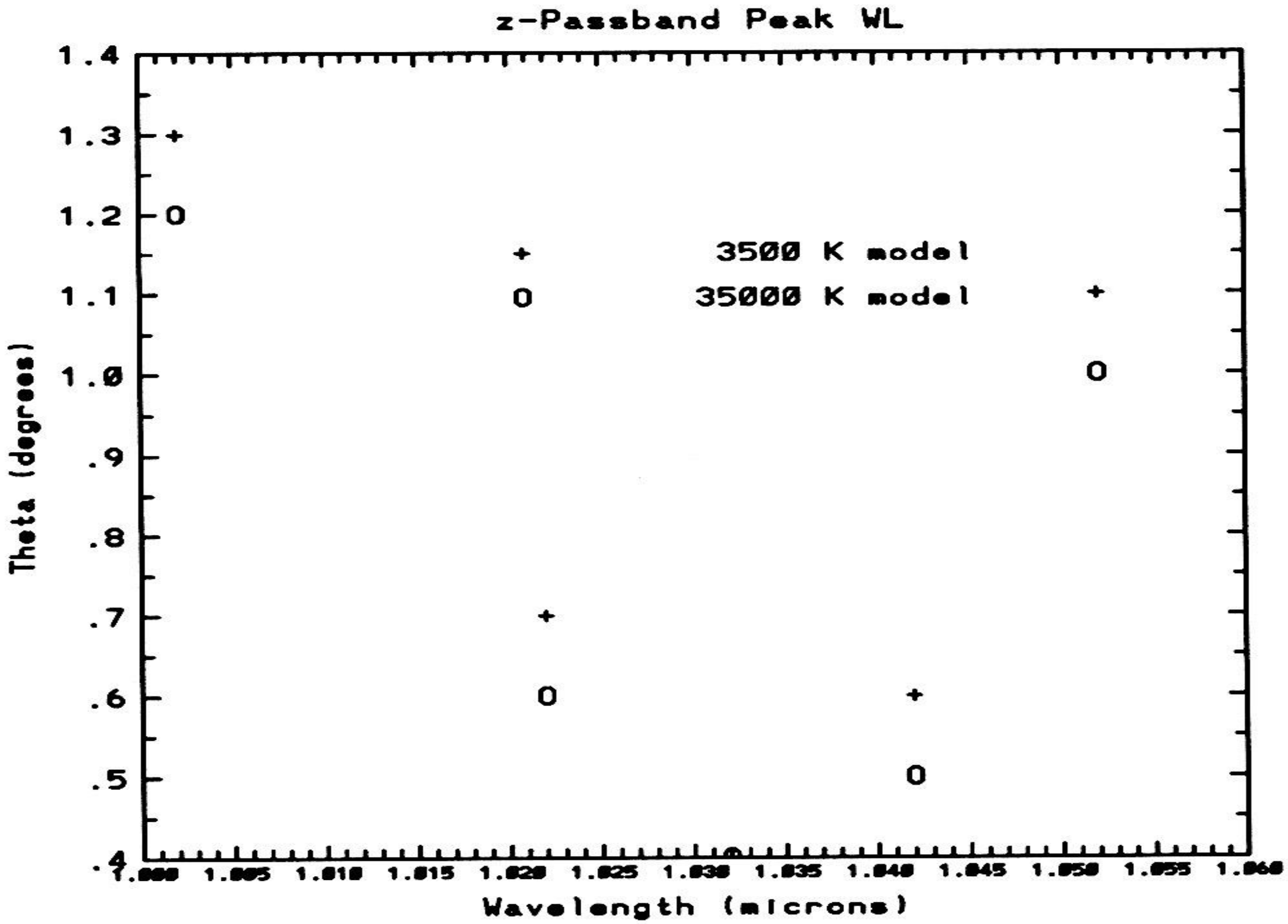

Fig. 10. a) Optimization curves for the placement of the proposed "z" passband. In this and other optimization plots, results are shown for two Kurucz stellar atmosphere models: T = 3500K, log g = 0 and T = 35000 K, log g = 4. The MODTRAN atmospheric model is for a site at 4.2 km at tropical latitudes, namely Mauna Kea

Optimized FWHM for iz passband

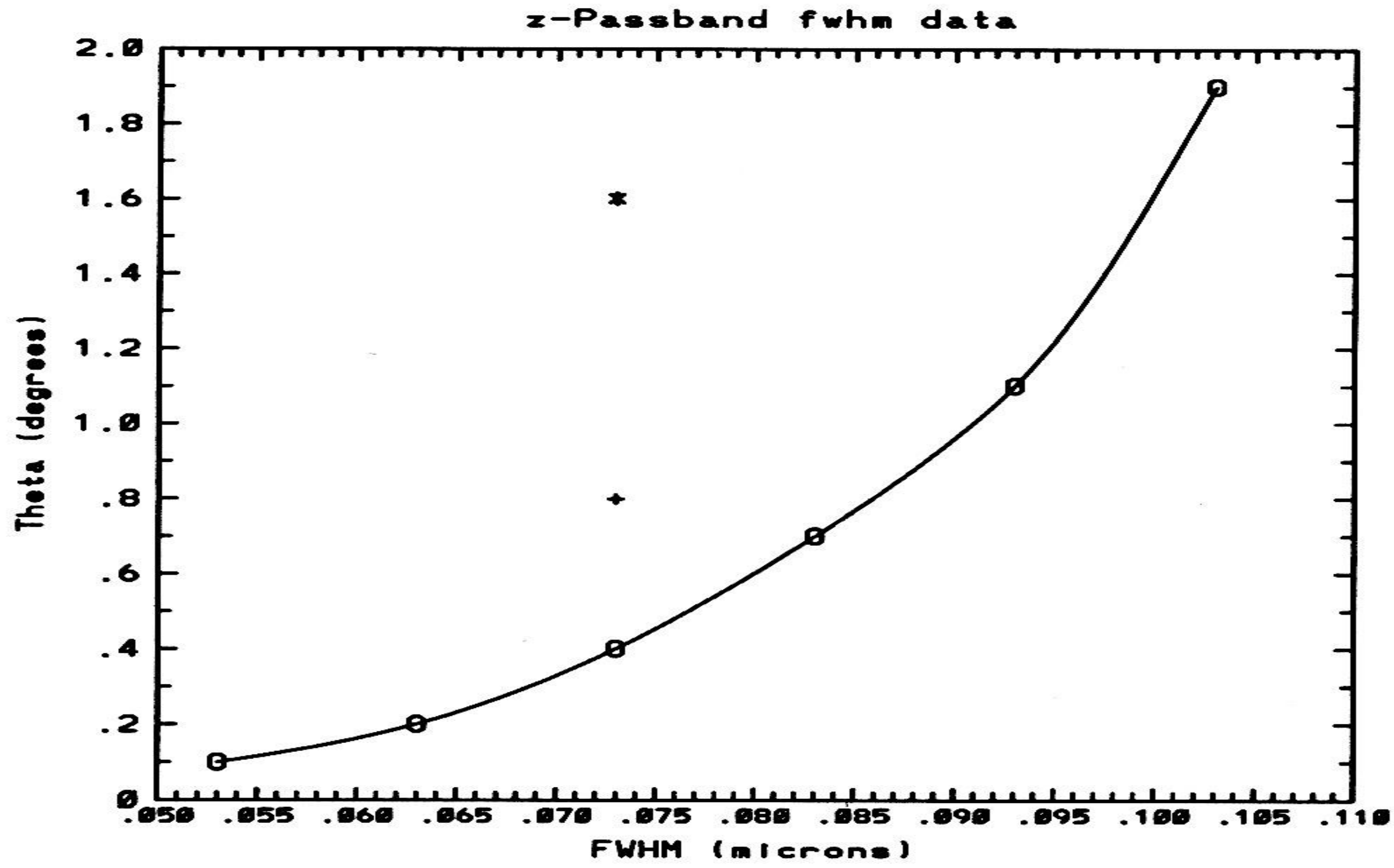

Fig. 10. b) Optimization data for the determination of $FWHM$ of the proposed "z" passband. Here as in several other plots, the data are virtually identical for the 3500 K and 35000 K sources and so are represented by the same symbols and lines. Results for triangular ("*") and trapezoidal ("+") passbands with the same $FWHM$ and peak wavelength, but for a summer, mid-latitude site at 1 km altitude, are also shown

Optimized passband for J window

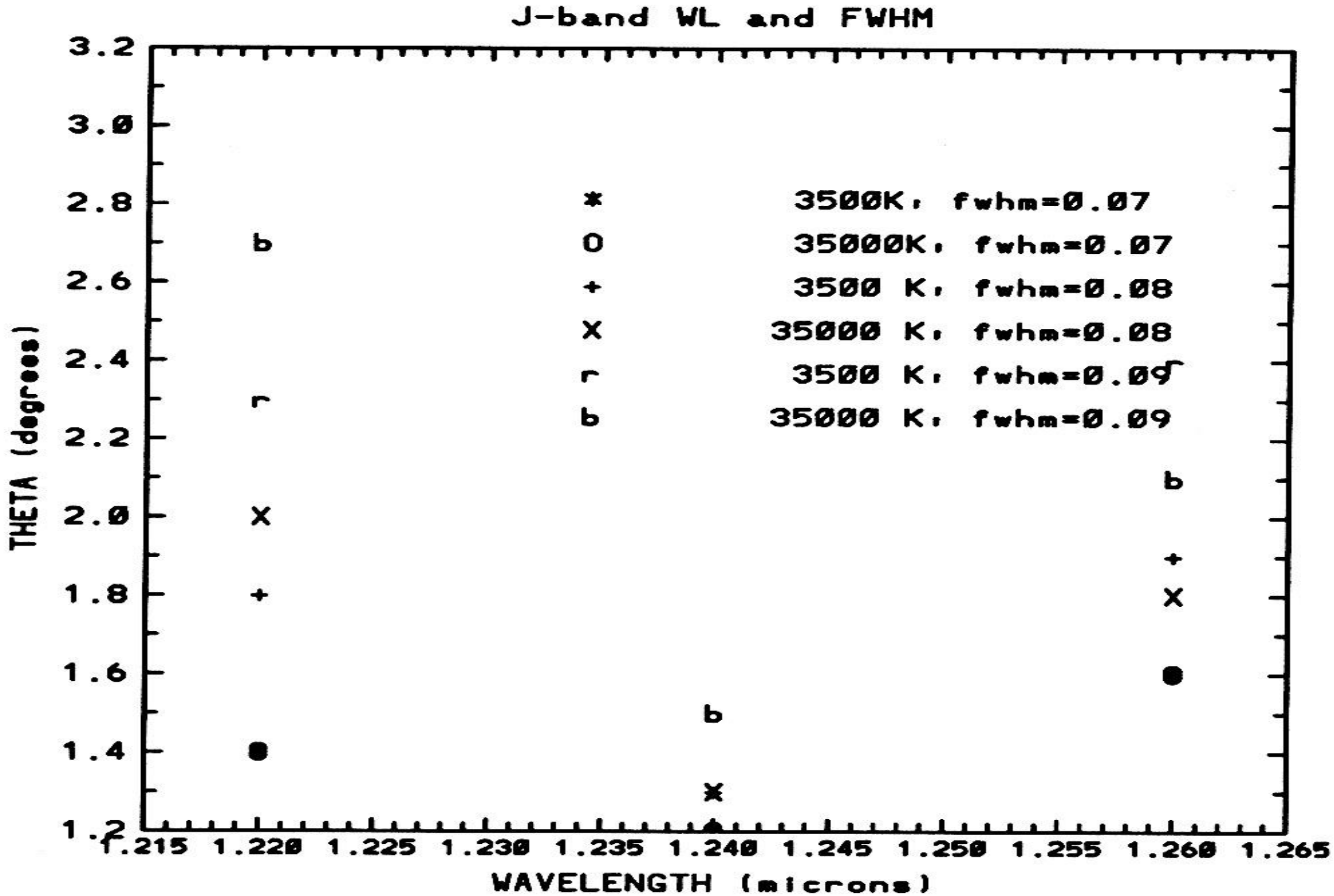

Fig. 11. Optimization data for the placement and *FWHM* determination of the proposed "*J*" passband. Note that the dispersion in θ with wavelength is minimal at 1.24 μm. These results are for a 4.2 km tropical atmosphere but the results for a 1 km atmosphere are quite similar

Optimized passband for H Window

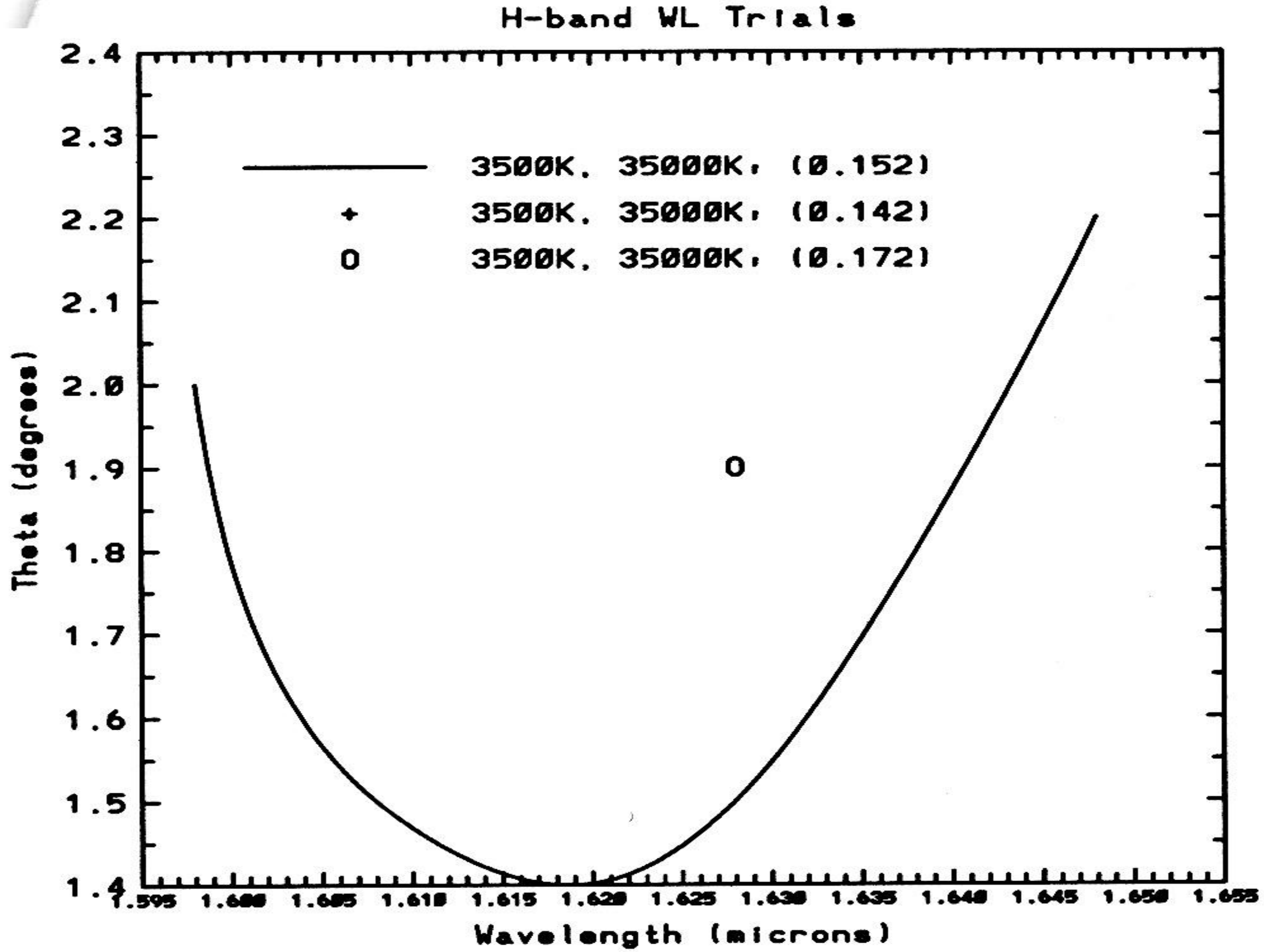

Fig. 13. a) Optimization curves for the placement of the proposed "*H*" passband. The results shown are for a 1 km, mid-latitude summer MODTRAN model, but results for higher altitude, drier sites are nearly identical

Optimized FWHM for iH passband

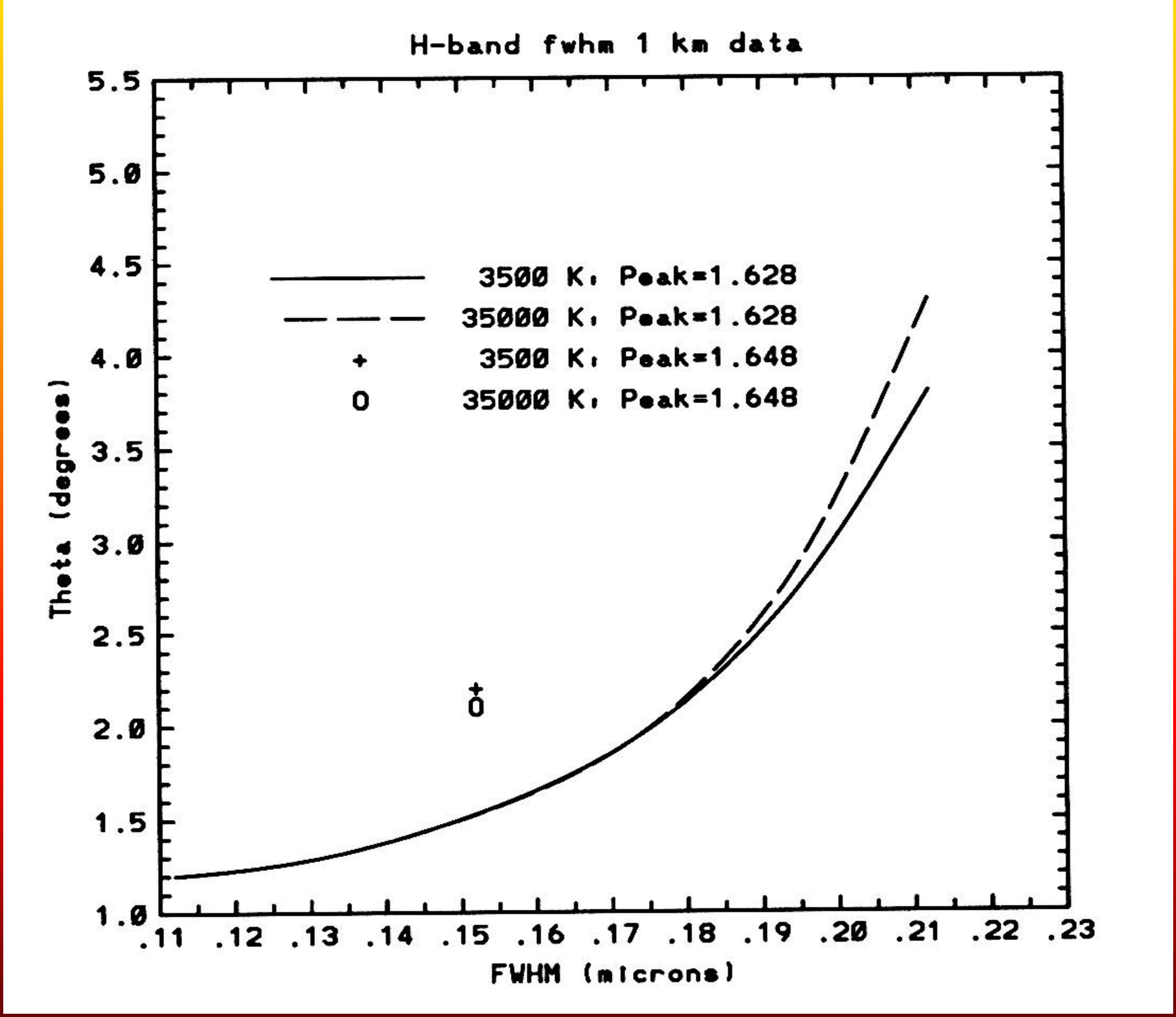

Emission & Transmission in H-window passbands

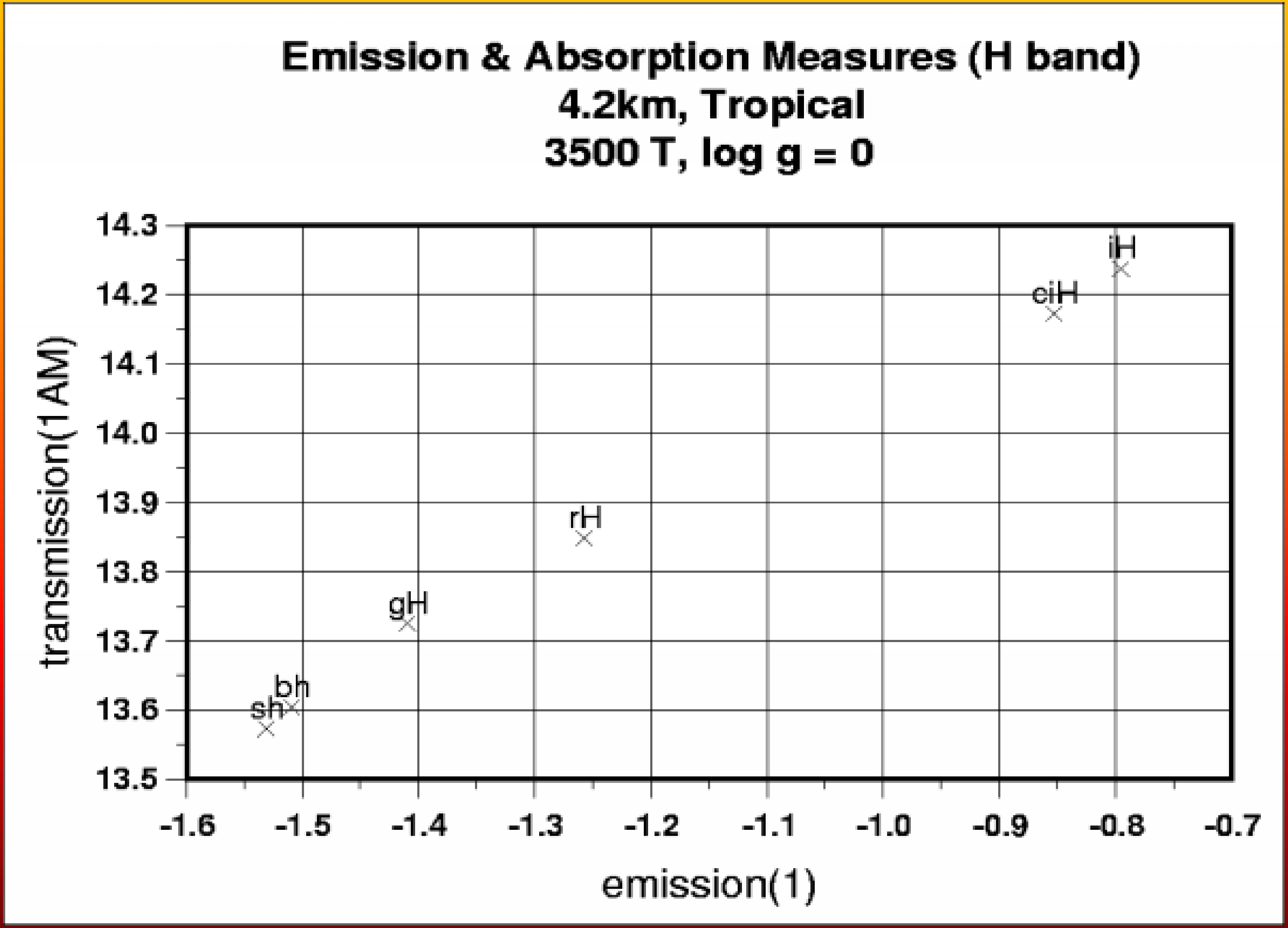

Optimized passband for K Window

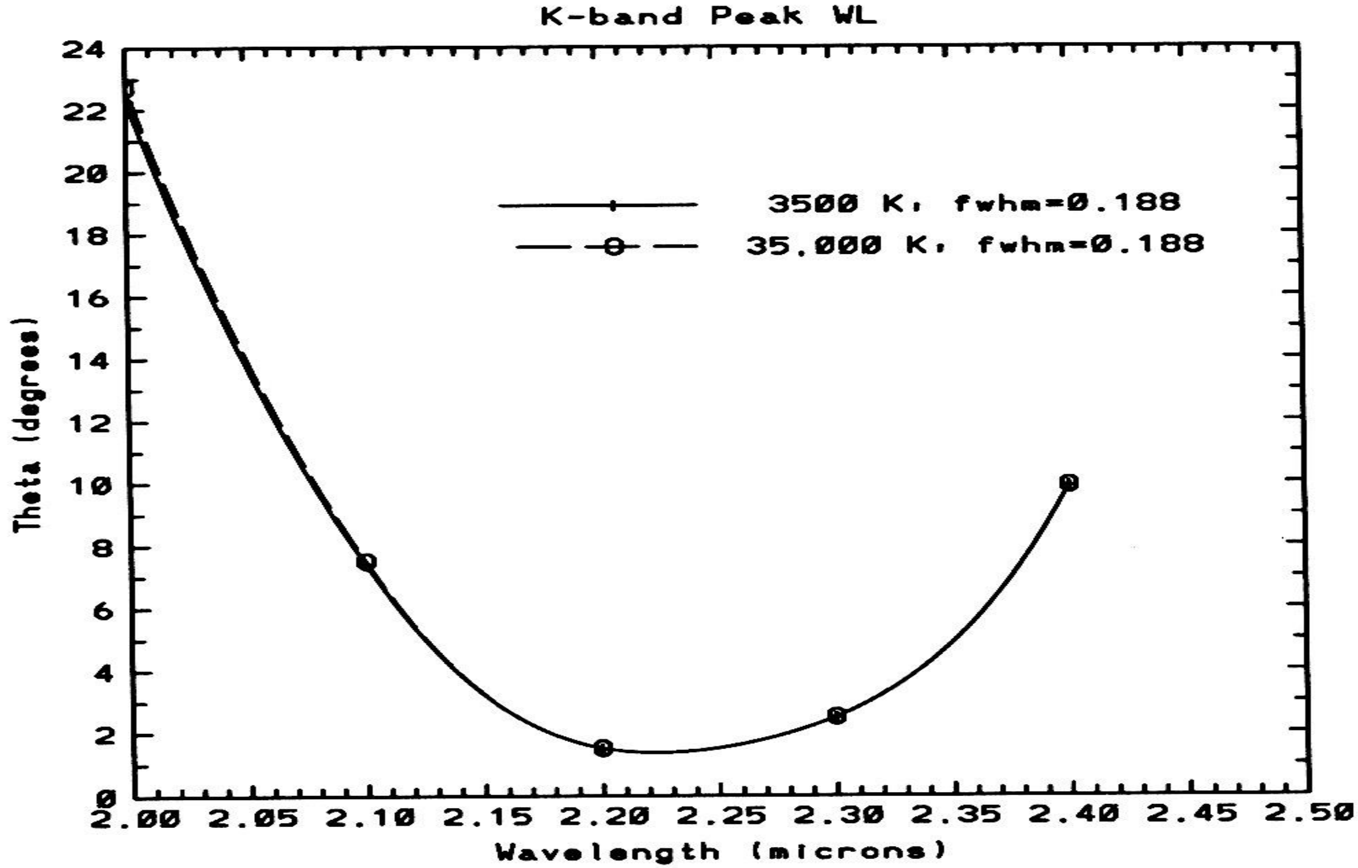

Fig. 15. a) Optimization curves for the placement of the proposed "K" passband for the tropical atmosphere at 4.2 km above sea level. The least θ value occurs for a passband close to 2.2 μm according to our simulations. We suggest a peak just to the blue of this minimum, at 2.196 μm to minimize thermal atmospheric emission in the bandpass. This passband will give an extinction curve nearly free of the Forbes effect

Optimized FWHM for iK passband

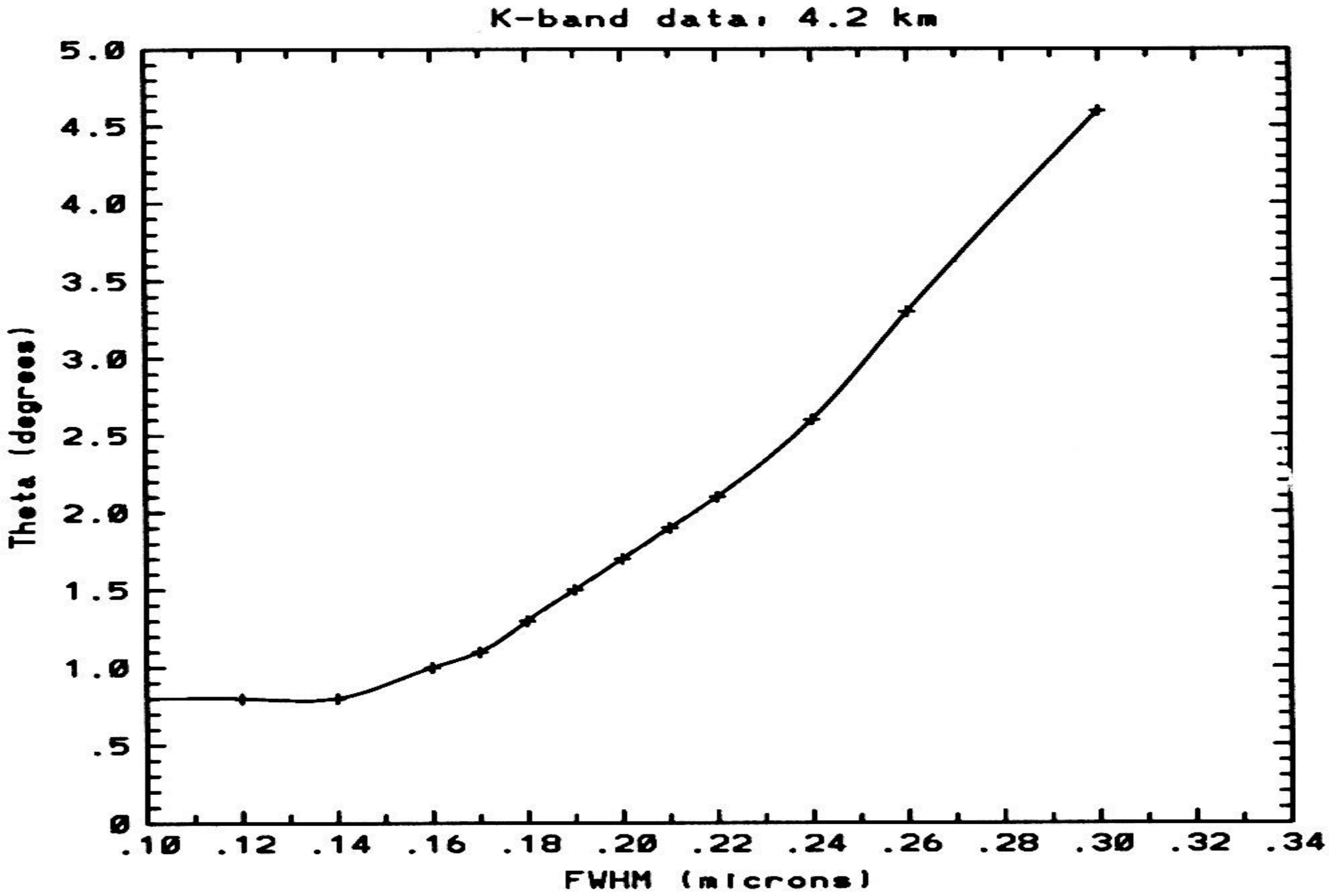

Fig. 15. b) Optimization data for the *FWHM* determination of the proposed "*K*" passband. The curve for the 4.2 km MODTRAN model rises more slowly than it does for the lower altitude sites. See the text for a description of how this passband differs from other K' passbands

Emission & Transmission in K-window passbands

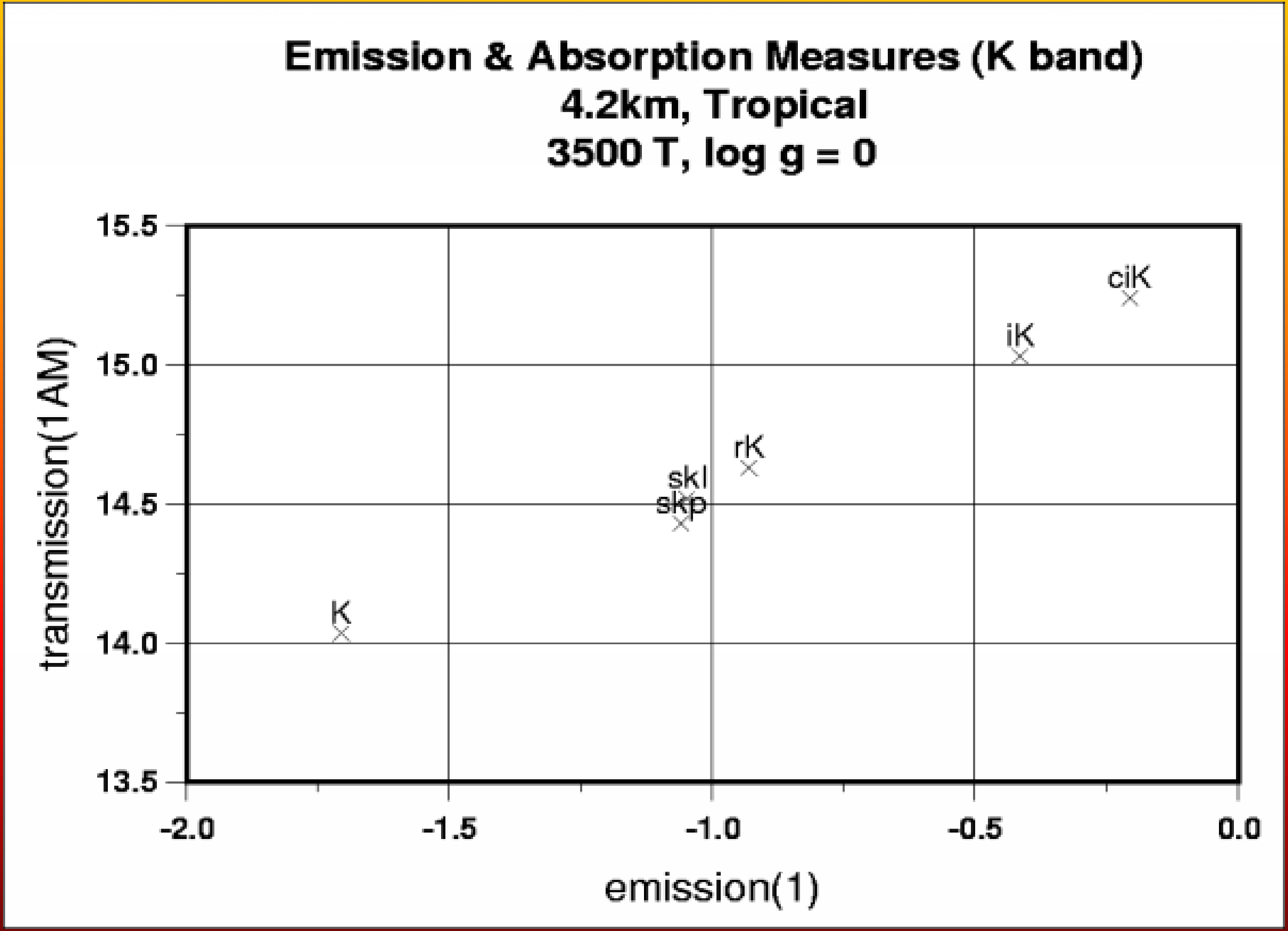

Optimized passband for L Window

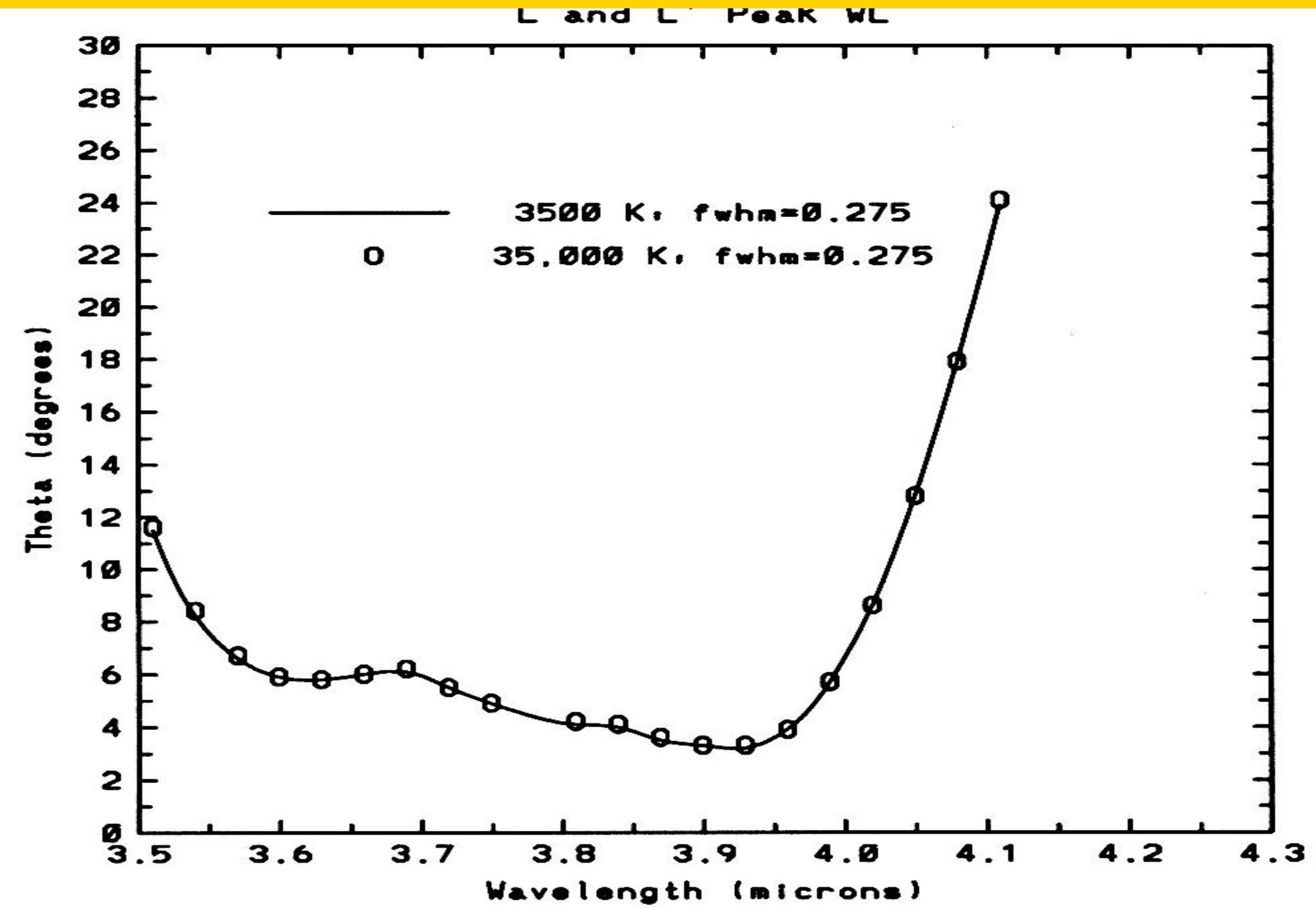

Fig. 17. a) Optimization curve for the placement of the proposed "L" and "L'" passbands. Results are shown for a 1 km, mid-latitude, summer model. The minimum suggests the advisability of at least two passbands, one near 3.6 and the other near 3.9 μm. Our suggested passbands overlap slightly

Optimized FWHM for iL passband

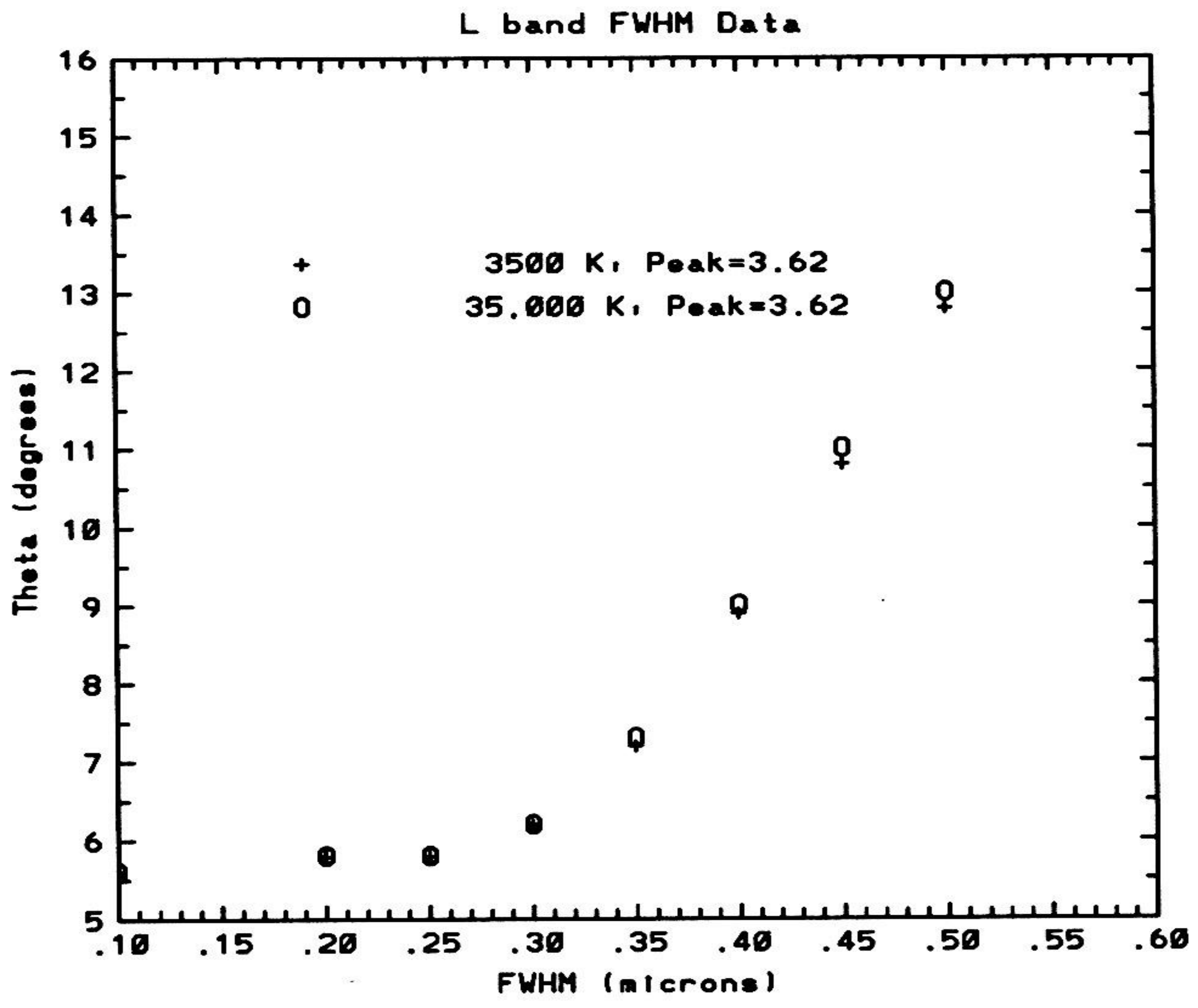

Fig. 17. b) Optimization data for the $FWHM$ determination of the proposed "L" passband

Optimized FWHM for iL' passband

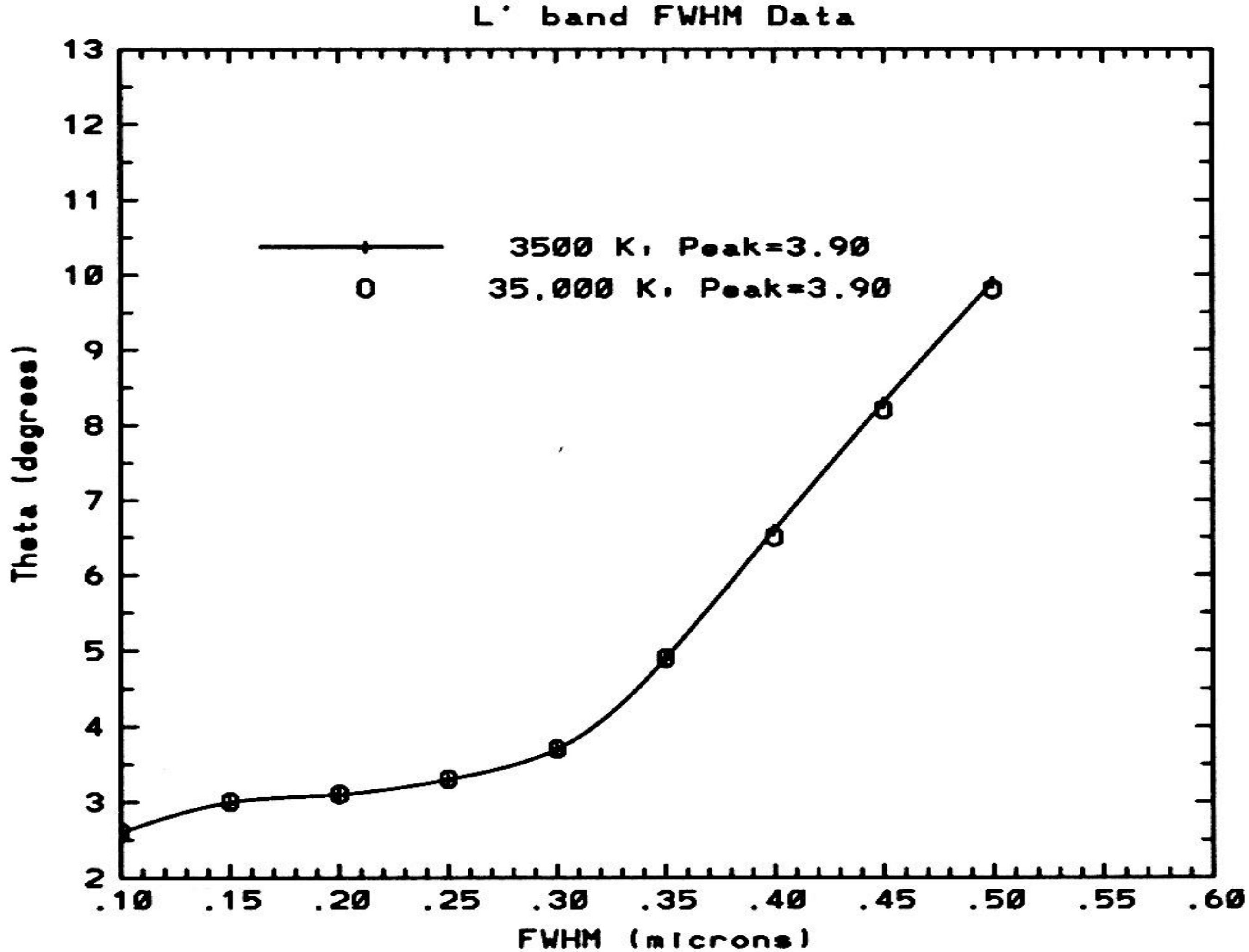

Fig. 17. c) Optimization data for the *FWHM* determination of the proposed "*L'* " passband in the cleaner part of the atmospheric window

Optimized passband for M Window

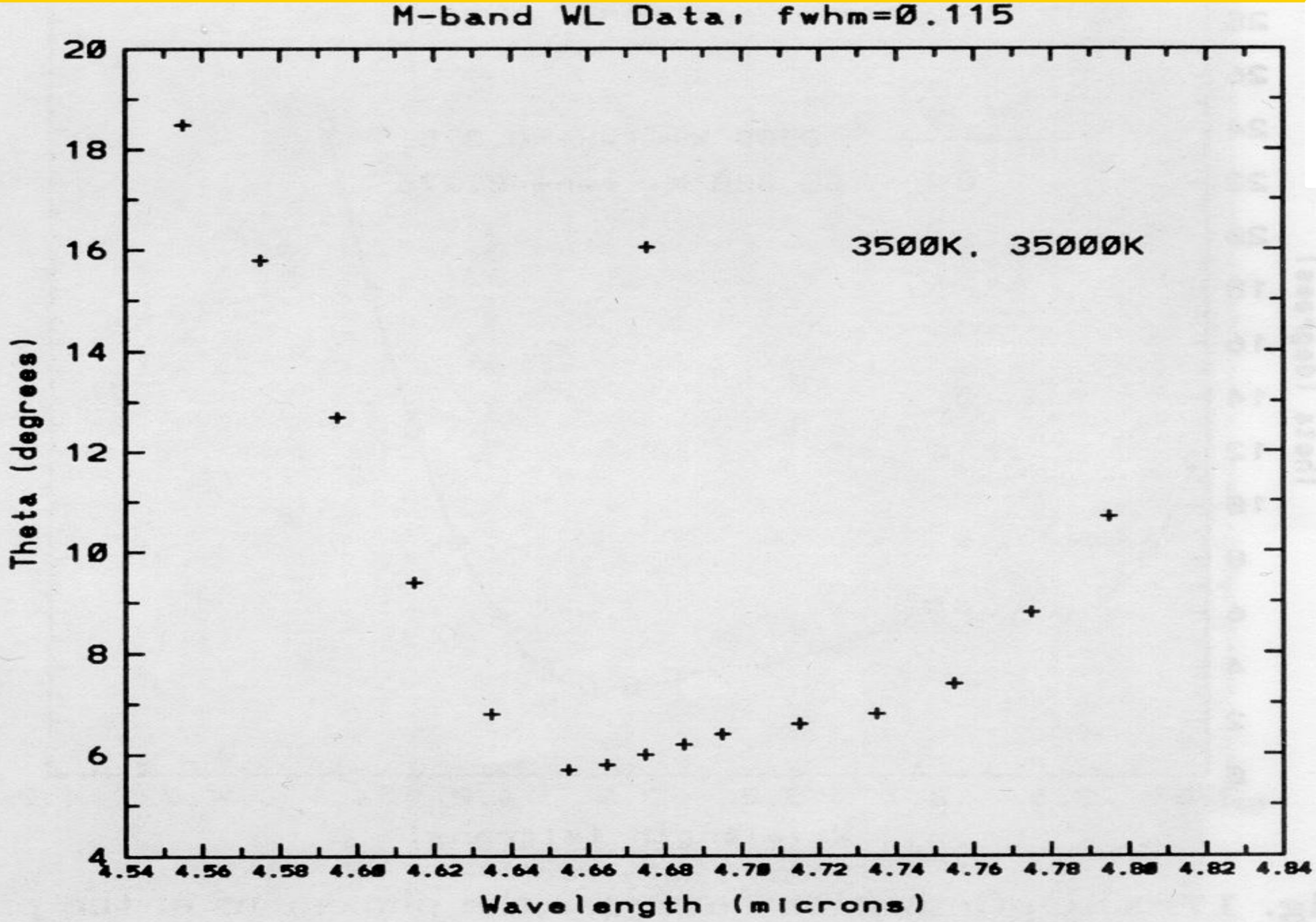

Fig. 19. a) Optimization curve for the placement of the proposed "*M*" passband for the tropical atmosphere at 4.2 km above sea level

Optimized FWHM for iM passband

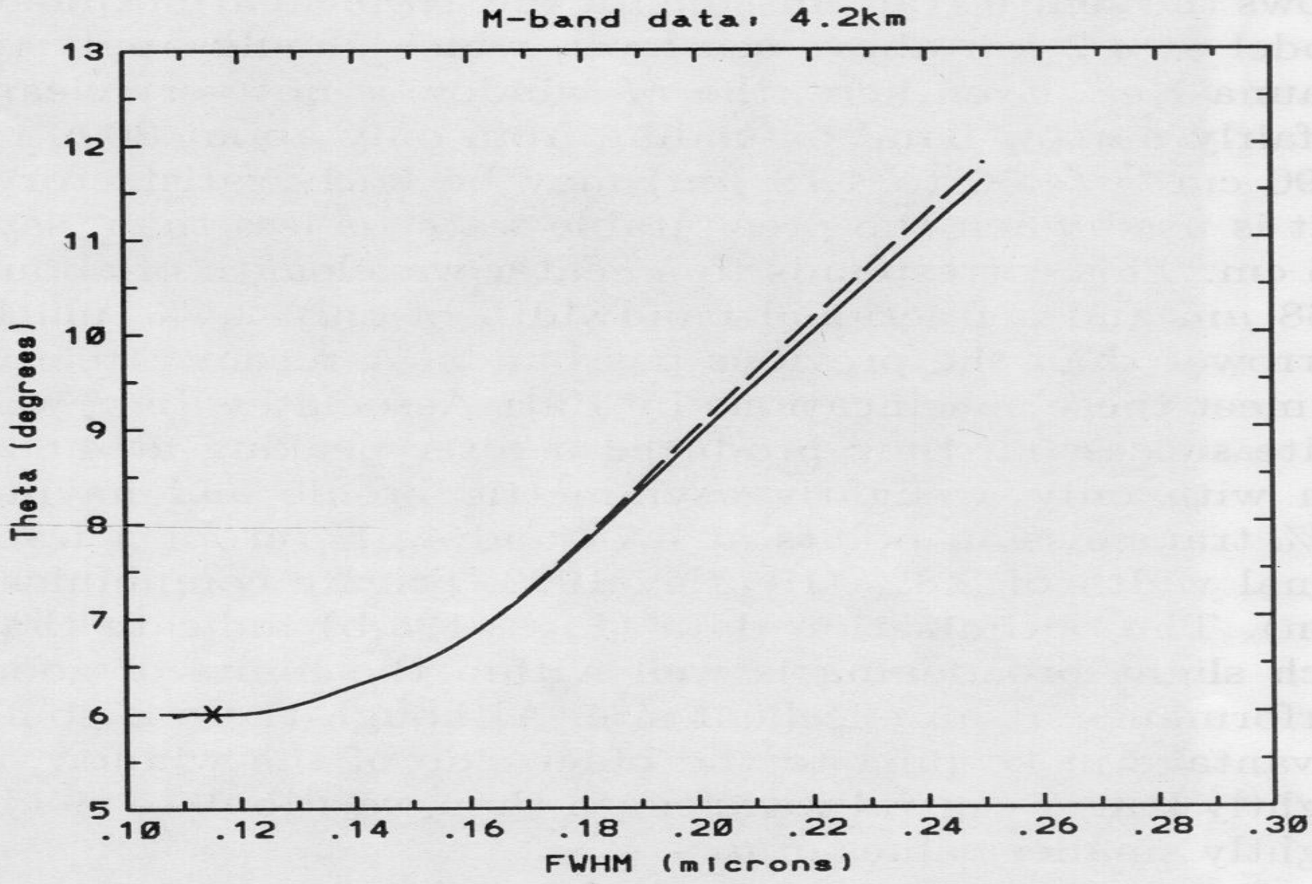

Fig. 19. b) Optimization data for the *FWHM* determination of the proposed "*M*" passband. The solid line is the response for a 3500 K dwarf, the dashed line that for a 35000 K giant. Note the identical results for the trapezoidal filter ("*x*"), which has the same peak (4.675 μm) and *FWHM* (0.114 μm) as the suggested triangular passband but also a flat maximum and slightly narrower base

Optimized passband for N Window

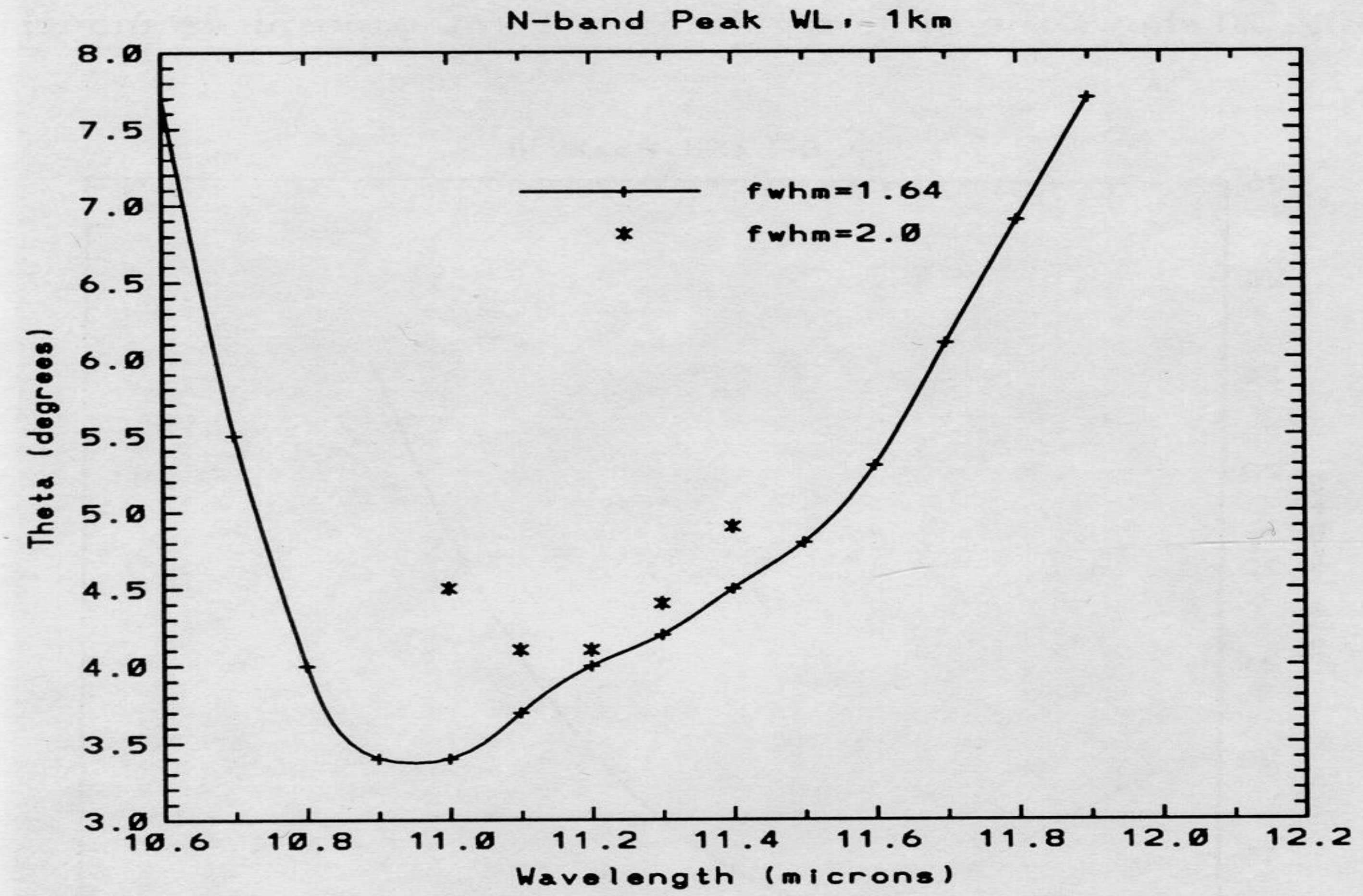

Fig. 21. a) Optimization curves for the placement of the proposed "*N*" passband. These results shown are for a 1 km mid-latitude site in summer. The curve is for a passband with $FWHM = 1.64\ \mu$m; other data are given for 2.0 ("*") μm $FWHM$

Optimized FWHM for iN passband

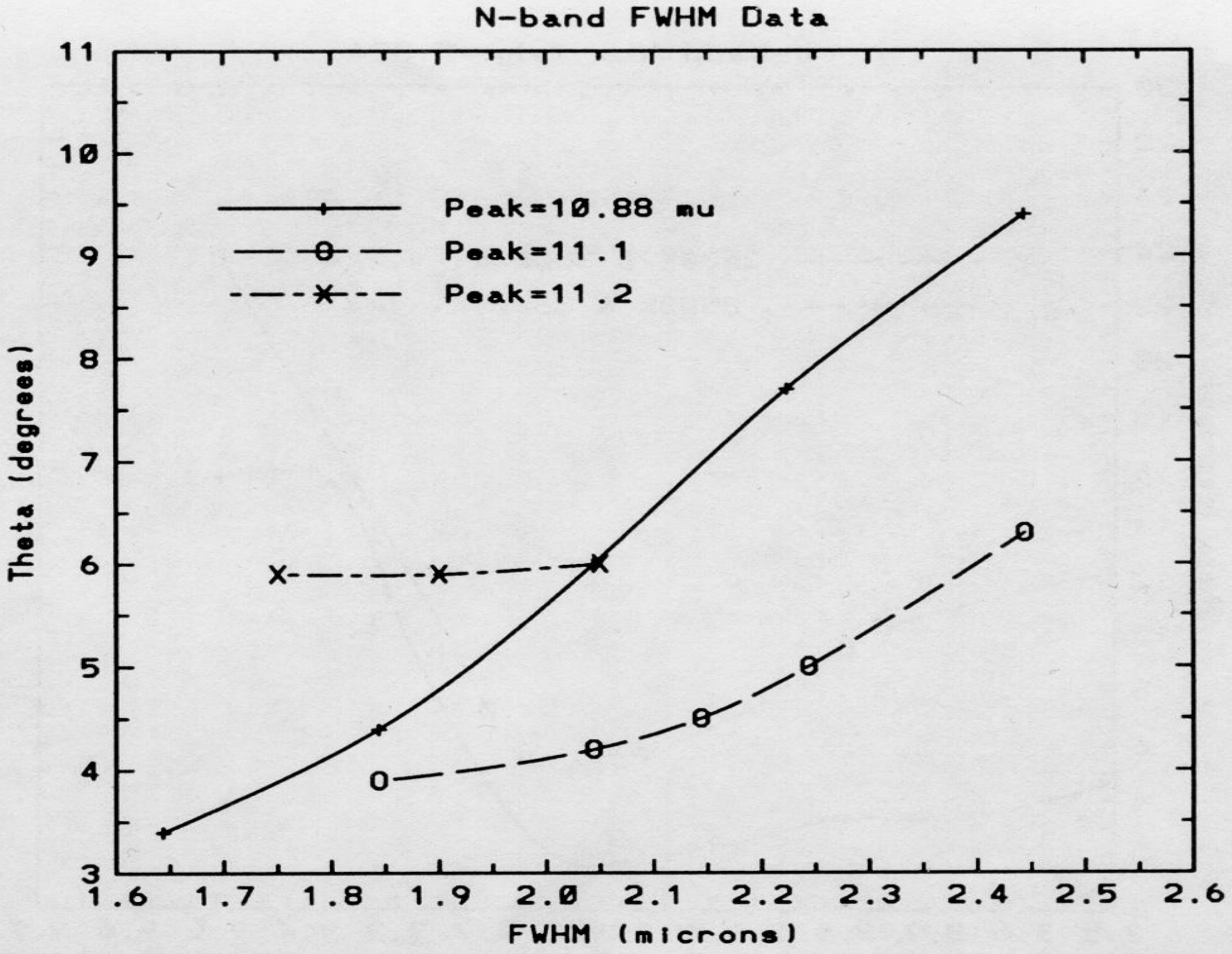

Fig. 21. b) Optimization data for the *FWHM* determination of the proposed "*N*" passband for several peak wavelength placements. Note that for *FWHM* values greater than about 1.7 μm, the lowest θ values are achieved for a peak wavelength of about 11.1 μm

Optimized passband for "n" Window

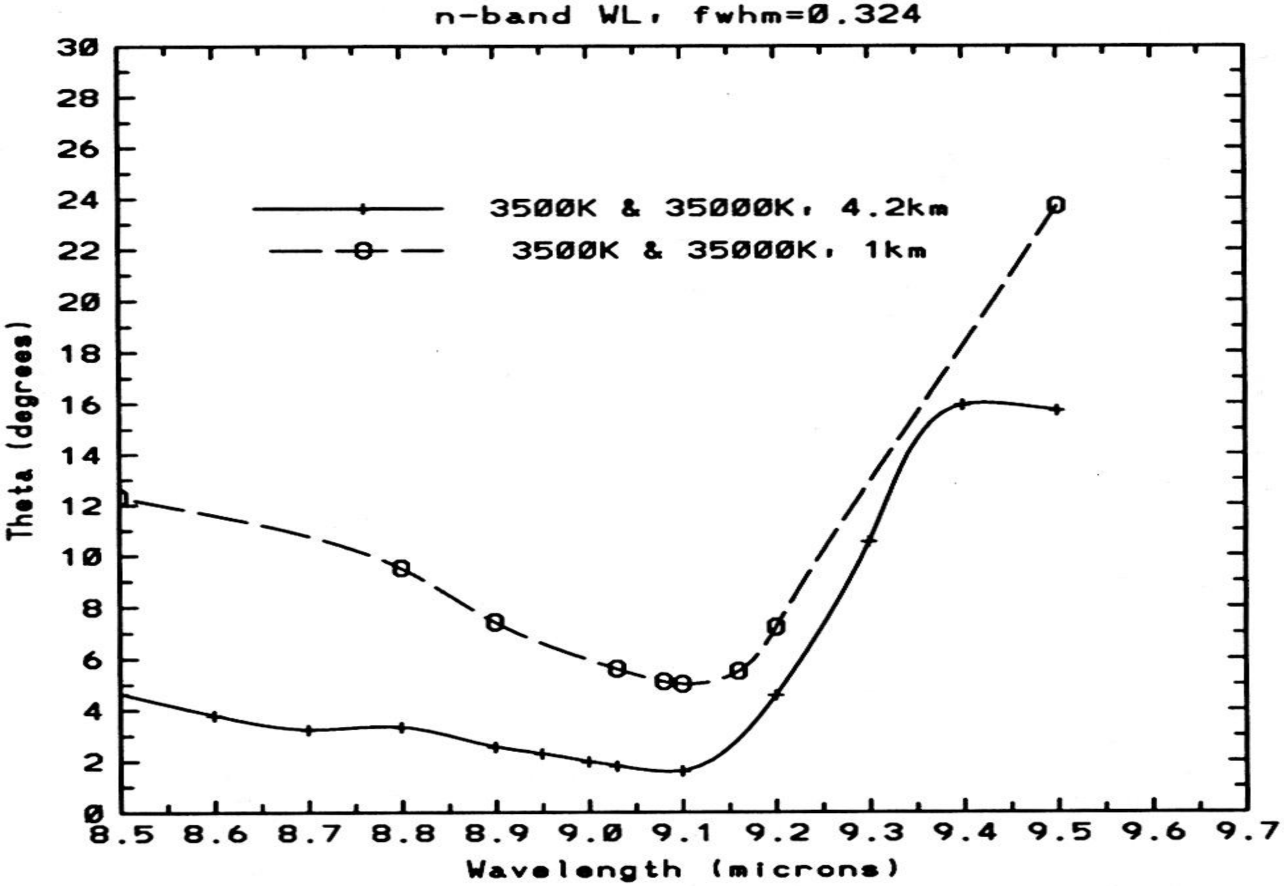

Fig. 22. a) Optimization curve for the placement of a proposed "*n*" passband. Although the deepest minimum occurs at 9.11 μm, θ rises rapidly at longer wavelengths so that we have suggested a peak wavelength closer to 9.0 μm (see Fig. 22b). Results for two terrestrial atmosphere models are shown

Optimized FWHM for in passband

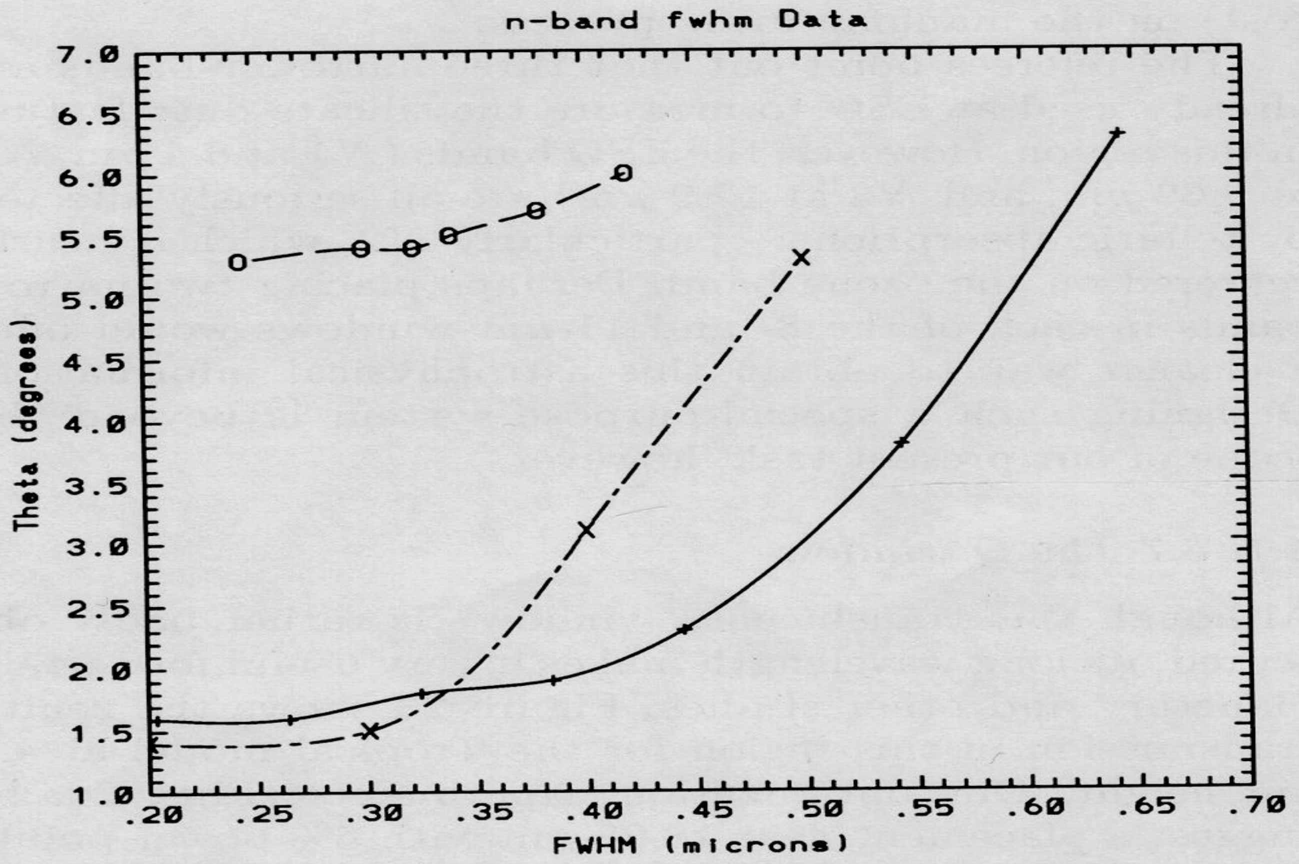

Fig. 22. b) Optimization data for the *FWHM* determination of a proposed "n" passband. Results are shown for both 4.2 km, tropical atmosphere and a 1 km, summer, mid-latitude atmosphere models. As in Fig. 22a, the differences for the two stellar sources are negligible. Note the increase in θ with *FWHM* beyond the apparent minimum for the passband peaking at 9.11 μm (x)

Optimized passband for Q Window